

# THE THICK-THIN DECOMPOSITION AND THE BILIPSCHITZ CLASSIFICATION OF NORMAL SURFACE SINGULARITIES

LEV BIRBRAIR, WALTER D NEUMANN, AND ANNE PICHON

ABSTRACT. We describe a natural decomposition of a normal complex surface singularity  $(X, 0)$  into its “thick” and “thin” parts. The former is essentially metrically conical, while the latter shrinks rapidly in thickness as it approaches the origin. The thin part is empty if and only if the singularity is metrically conical; the link of the singularity is then Seifert fibered. In general the thin part will not be empty, in which case it always carries essential topology. Our decomposition has some analogy with the Margulis thick-thin decomposition for a negatively curved manifold. However, the geometric behavior is very different; for example, often most of the topology of a normal surface singularity is concentrated in the thin parts.

By refining the thick-thin decomposition, we then give a complete description of the intrinsic bilipschitz geometry of  $(X, 0)$  in terms of its topology and a finite list of numerical bilipschitz invariants.

## 1. INTRODUCTION

Lipschitz geometry of singular spaces is an intensively developing subject. In [11] R. Hardt and D. Sullivan considered Lipschitz geometry in their study of Whitney stratifications of complex algebraic varieties. D. Sullivan conjectured that the set of Lipschitz structures is tame, i.e., the set of the equivalence classes complex algebraic sets in  $\mathbb{C}^n$ , defined by polynomials of the degree less or equal to  $k$  is finite. T. Mostowski [25] proved this conjecture, but the proof does not show how to describe the equivalence classes. For the case of complex plane curves the classes were described by Pham and Teissier [32] and Fernandes [10]. They show that the embedded Lipschitz geometry of plane curves is determined by the topology. The case of complex algebraic surfaces is much richer and is the case we study here.

Let  $(X, 0)$  be the germ of a normal complex surface singularity. Given an embedding  $(X, 0) \subset (\mathbb{C}^n, 0)$ , the standard hermitian metric on  $\mathbb{C}^n$  induces a metric on  $X$  given by arc-length of curves in  $X$  (the so-called “inner metric”). Up to bilipschitz equivalence this metric is independent of the choice of embedding in affine space.

It is well known that for all sufficiently small  $\epsilon > 0$  the intersection of  $X$  with the sphere  $S_\epsilon \subset \mathbb{C}^n$  about 0 of radius  $\epsilon$  is transverse, and the germ  $(X, 0)$  is therefore “topologically conical,” i.e., homeomorphic to the cone on its link  $X \cap S_\epsilon$  (in fact, this is true for any semi-algebraic germ). However,  $(X, 0)$  need not be “metrically conical” (bilipschitz equivalent to a standard metric cone), as was first shown in [2]. In [3, 4, 5] it is shown that failure of metric conicalness is common, and in [5]

---

1991 *Mathematics Subject Classification.* 14B05, 32S25, 32S05, 57M99.

*Key words and phrases.* bilipschitz geometry, normal surface singularity, thick-thin decomposition.

it is also shown that bilipschitz geometry of a singularity may not be determined by its topology.

In those papers the failure of metric conicalness and differences in bilipschitz geometry were determined by local obstructions: existence of topologically non-trivial subsets of the link of the singularity (“fast loops” and “separating sets”) whose size shrinks faster than linearly as one approaches the origin.

In this paper we first describe a natural decomposition of the germ  $(X, 0)$  into two parts, the *thick* and the *thin* parts, such that the thin part carries all the “non-trivial” bilipschitz geometry and we later refine this to give a classification of the bilipschitz structure. Our thick-thin decomposition is somewhat analogous to the Margulis thick-thin decomposition of a negatively curved manifold, where the thin part consists of points  $p$  which lie on a closed essential loop of length  $\leq 2\eta$  for some small  $\eta$ . A (rough) version of our thin part can be defined similarly using essential loops in  $X \setminus \{0\}$ , and length bound of the form  $\leq |p|^{1+c}$  for some small  $c$ . We return to this in section 8.

**Definition 1.1** (Thin). A semialgebraic germ  $(Z, 0) \subset (\mathbb{R}^N, 0)$  of pure dimension  $k$  is *thin* if its tangent cone  $T_0Z$  has dimension strictly less than  $k$ .

This definition only depends on the inner metric of  $Z$  and not on the embedding in  $\mathbb{R}^N$ . Indeed, instead of  $T_0Z$  one can use the metric tangent cone  $\mathcal{T}_0Z$  of Bernig and Lytchak in the definition, since it is a bilipschitz invariant for the inner metric and maps finite-to-one to  $T_0Z$  (see [1]). The metric tangent cone is discussed further in Section 9, where we show that it can be recovered from the thick-thin decomposition.

**Definition 1.2** (Thick). Let  $B_\epsilon \subset \mathbb{R}^N$  denote the ball of radius  $\epsilon$  centered at the origin, and  $S_\epsilon$  its boundary. A semialgebraic germ  $(Y, 0) \subset (\mathbb{R}^N, 0)$  is *thick* if there exists  $\epsilon_0 > 0$  and  $K \geq 1$  such that  $Y \cap B_{\epsilon_0}$  is the union of subsets  $Y_\epsilon$ ,  $\epsilon \leq \epsilon_0$  which are metrically conical with bilipschitz constant  $K$  and satisfy the following properties:

- (1)  $Y_\epsilon \subset B_\epsilon$ ,  $Y_\epsilon \cap S_\epsilon = Y \cap S_\epsilon$  and  $Y_\epsilon$  is metrically conical as a cone on its link  $Y \cap S_\epsilon$ .
- (2) For  $\epsilon_1 < \epsilon_2$  we have  $Y_{\epsilon_2} \cap B_{\epsilon_1} \subset Y_{\epsilon_1}$  and this embedding respects the conical structures. Moreover, the difference  $(Y_{\epsilon_1} \cap S_{\epsilon_1}) \setminus (Y_{\epsilon_2} \cap S_{\epsilon_1})$  of the links of these cones is homeomorphic to  $\partial(Y_{\epsilon_1} \cap S_{\epsilon_1}) \times [0, 1)$ .

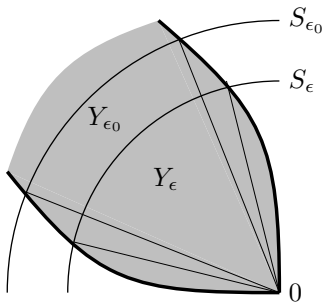


FIGURE 1. Thick germ

Clearly, a semi-algebraic germ cannot be both thick and thin. The following proposition helps picture “thinness”. Although it is well known, we give a quick proof in Section 5 for convenience.

**Proposition 1.3.** *A semialgebraic germ  $(Z, 0) \subset (\mathbb{R}^N, 0)$  is contained in a “horn neighborhood” of its tangent cone  $T_0Z$ . In other words, there exist  $\epsilon_0 > 0$ ,  $c > 0$  and  $q > 1$  such that  $Z \cap B_\epsilon$  is contained in a  $c\epsilon^q$ -neighborhood of  $T_0Z \cap B_\epsilon$  for all  $\epsilon \leq \epsilon_0$ .*

For example, the set  $Z = \{(x, y, z) \in \mathbb{R}^3 : x^2 + y^2 \leq z^3\}$  gives a thin germ at 0 since it is a 3-dimensional germ whose tangent cone is the  $z$ -axis. The intersection  $Z \cap B_\epsilon$  is contained in a closed  $\epsilon^{3/2}$ -neighborhood of the  $z$ -axis. The complement in  $\mathbb{R}^3$  of this thin set is thick.

For any subgerm  $(A, 0)$  of  $(\mathbb{C}^n, 0)$  or  $(\mathbb{R}^N, 0)$  we write

$$A^{(\epsilon)} := A \cap S_\epsilon \subset S_\epsilon.$$

In particular, when  $A$  is semialgebraic and  $\epsilon$  is sufficiently small,  $A^{(\epsilon)}$  is the  $\epsilon$ -link of  $(A, 0)$ .

**Definition 1.4** (Thick-thin decomposition). A *thick-thin decomposition* of the normal complex surface germ  $(X, 0)$  is a decomposition of it as a union of germs of pure dimension 4:

$$(X, 0) = \bigcup_{i=1}^r (Y_i, 0) \cup \bigcup_{j=1}^s (Z_j, 0),$$

such that the  $Y_i \setminus \{0\}$  and  $Z_j \setminus \{0\}$  are connected and:

- (1) Each  $Y_i$  is thick and each  $Z_j$  is thin.
- (2) The  $Y_i \setminus \{0\}$  are pairwise disjoint and the  $Z_j \setminus \{0\}$  are pairwise disjoint.
- (3) If  $\epsilon_0$  is chosen small enough that  $S_\epsilon$  is transverse to each of the germs  $(Y_i, 0)$  and  $(Z_j, 0)$  for  $\epsilon \leq \epsilon_0$  then  $X^{(\epsilon)} = \bigcup_{i=1}^r Y_i^{(\epsilon)} \cup \bigcup_{j=1}^s Z_j^{(\epsilon)}$  decomposes the 3-manifold  $X^{(\epsilon)} \subset S_\epsilon$  into connected submanifolds with boundary, glued along their boundary components.

We call the links  $Y_i^{(\epsilon)}$  and  $Z_j^{(\epsilon)}$  of the thick and thin pieces *thick and thin zones* of the link  $X^{(\epsilon)}$ .

**Definition 1.5.** A thick-thin decomposition is *minimal* if

- (1) the tangent cone of its thin part  $\bigcup_{j=1}^s Z_j$  is contained in the tangent cone of the thin part of any other thick-thin decomposition and
- (2) the number of its thin pieces is minimal among thick-thin decompositions satisfying (1).

The following theorems express the existence and uniqueness of thick-thin decompositions for normal complex surface germs.

**Theorem 1.6** (Existence). *There exists a minimal thick-thin decomposition  $(X, 0) = \bigcup_{i=1}^r (Y_i, 0) \cup \bigcup_{j=1}^s (Z_j, 0)$ . It satisfies  $r \geq 1$ ,  $s \geq 0$  and has the following properties for  $0 < \epsilon \leq \epsilon_0$ :*

- (1) Each thick zone  $Y_i^{(\epsilon)}$  is a Seifert fibered manifold.
- (2) Each thin zone  $Z_j^{(\epsilon)}$  is a graph manifold (union of Seifert manifolds glued along boundary components).

- (3) *There exist constants  $c_j > 0$  and  $q_j > 1$  and fibrations  $\zeta_j^{(\epsilon)}: Z_j^{(\epsilon)} \rightarrow S^1$  depending smoothly on  $\epsilon \leq \epsilon_0$  such that the fibers  $\zeta_j^{-1}(t)$  have diameter at most  $c_j \epsilon^{q_j}$  (we call these fibers the Milnor fibers of  $Z_j^{(\epsilon)}$ ).*

This decomposition is constructed in Section 2 and its minimality is proved in Lemma 8.1. The following uniqueness theorem is proved in Section 8.

**Theorem 1.7** (Uniqueness). *Any minimal thick-thin decomposition of  $(X, 0)$  is isotopic to any other minimal thick-thin decomposition. In particular, it has the properties described in the previous theorem.*

This equivalence of thick-thin decompositions is not necessarily bilipschitz; for example one can always find one with smaller  $q_j$ 's. But the bilipschitz classification which we describe later leads to a “best” minimal thick-thin decomposition, which is unique up to bilipschitz equivalence.

We will take a resolution approach to construct the thick-thin decomposition, but another way of constructing it is as follows. Recall (see [34, 23]) that a line  $L$  tangent to  $X$  at 0 is *exceptional* if the limit at 0 of tangent planes to  $X$  along a curve in  $X$  tangent to  $L$  at 0 depends on the choice of this curve. Just finitely many tangent lines to  $X$  at 0 are exceptional. To obtain the thin part one intersects  $X \setminus \{0\}$  with a  $q$ -horn disk-bundle neighborhood of each exceptional tangent line  $L$  for  $q > 1$  sufficiently small and then discards any “trivial” components of these intersections (those whose closures are locally just cones on solid tori; such trivial components arise also in our resolution approach, and showing that they can be absorbed into the thick part takes some effort).

In [3] a *fast loop* is defined as a family of closed curves in the links  $X^{(\epsilon)} := X \cap S_\epsilon$ ,  $0 < \epsilon \leq \epsilon_0$ , depending continuously on  $\epsilon$ , which are not homotopically trivial in  $X^{(\epsilon)}$  but whose lengths are proportional to  $\epsilon^k$  for some  $k > 1$ , and it is shown that these are obstructions to metric conicalness<sup>1</sup>

In Theorem 7.5 we show

**Theorem (7.5).** *Each thin piece  $Z_j$  contains fast loops. In fact, each boundary component of its Milnor fiber gives a fast loop.*

**Corollary 1.8.** *The following are equivalent, and each implies that the link of  $(X, 0)$  is Seifert fibered:*

- (1)  $(X, 0)$  is metrically conical;
- (2)  $(X, 0)$  has no fast loops;
- (3)  $(X, 0)$  has no thin piece (so it consists of a single thick piece).

**Bilipschitz classification.** Building on the thin-thick decomposition, we give a complete classification of the geometry of  $(X, 0)$  up to bilipschitz equivalence. We describe this geometry in terms of a decomposition of  $(X, 0)$  as a union of semi-algebraic germs. We will describe this decomposition, which refines the thick-thin decomposition, in terms of the decomposition of the link  $X^{(\epsilon)}$ .

We first refine the decomposition  $X^{(\epsilon)} = \bigcup_{i=1}^r Y_i^{(\epsilon)} \cup \bigcup_{j=1}^s Z_j^{(\epsilon)}$  by decomposing each thin zone  $Z_j^{(\epsilon)}$  into its JSJ decomposition (minimal decomposition into Seifert

<sup>1</sup>We later call these *fast loops of the first kind*, since in section 7 we define a related concept of *fast loop of the second kind* and show these also obstruct metric conicalness.

fibered manifolds glued along their boundaries), while leaving the thick zones  $Y_i^{(\epsilon)}$  as they are. We then thicken some of the gluing tori of this refined decomposition to collars  $T^2 \times I$ , to add some extra “annular” pieces (the choice where to do this is described in Section 10). At this point we have  $X^{(\epsilon)}$  glued together from various Seifert fibered manifolds (in general not the minimal such decomposition).

Let  $\Gamma_0$  be the decomposition graph for this, with a vertex for each piece and edge for each gluing torus, so we can write this decomposition as

$$(1) \quad X^{(\epsilon)} = \bigcup_{\nu \in V(\Gamma_0)} M_\nu^{(\epsilon)},$$

where  $V(\Gamma_0)$  is the vertex set of  $\Gamma_0$ .

**Theorem 1.9** (Classification Theorem). *The bilipschitz geometry of  $(X, 0)$  determines and is uniquely determined by the following data:*

- (1) *The decomposition of  $X^{(\epsilon)}$  into Seifert fibered manifolds as described above, refining the thick-thin decomposition;*
- (2) *for each thin zone  $Z_j^{(\epsilon)}$ , the unoriented isotopy class of the foliation by fibers of the fibration  $\zeta_j^{(\epsilon)}: Z_j^{(\epsilon)} \rightarrow S^1$  (see Theorem 1.6(3));*
- (3) *for each vertex  $\nu \in V(\Gamma_0)$ , a rational weight  $q_\nu \geq 1$  with  $q_\nu = 1$  if and only if  $M_\nu^{(\epsilon)}$  is a  $Y_i^{(\epsilon)}$  (i.e., a thick zone) and with  $q_\nu \neq q_{\nu'}$  if  $\nu$  and  $\nu'$  are adjacent vertices.*

In item (2) we ask for the foliation by fibers rather than the fibration itself since we do not want to distinguish fibrations  $\zeta: Z \rightarrow S^1$  which become equivalent after composing each with a covering maps  $S^1 \rightarrow S^1$ . Note that item (2) describes discrete data, since the foliation is determined up to isotopy by a primitive element of  $H^1(Z_j^{(\epsilon)}; \mathbb{Z})$  up to sign.

The proof of the theorem is in terms of a canonical “bilipschitz model”

$$(2) \quad \widehat{X} = \bigcup_{\nu \in V(\Gamma_0)} \widehat{M}_\nu \cup \bigcup_{\sigma \in E(\Gamma_0)} \widehat{A}_\sigma,$$

with  $\widehat{X} \cong X \cap B_\epsilon$  (bilipschitz) and where each  $\widehat{A}_\sigma$  is a collar (cone on a toral annulus  $T^2 \times I$ ) while each  $\widehat{M}_\nu$  is homeomorphic to the cone on  $M_\nu^{(\epsilon)}$ . The pieces carry Riemannian metrics determined by the  $q_\nu$ ’s and the foliation data of the theorem; these metrics are global versions of the local metrics used by Hsiang and Pati [15] and Nagase [30]. On a piece  $\widehat{M}_\nu$  the metric is what Hsiang and Pati call a “Cheeger type metric” (locally of the form  $dr^2 + r^2 d\theta^2 + r^{2q_\nu} (dx^2 + dy^2)$ ; see Definitions 11.2, 11.3). On a piece  $\widehat{A}_\sigma$  it has a Nagase type metric as described in Nagase’s correction to [15] (see Definition 11.1).

In this work we develop some results we need about polar curves which may be of independent interest. In Proposition 3.2 and later we contribute to the question of where the polar curves are located (see, e.g., [34] for a discussion). In particular each thin piece contains a polar curve (component of the singular locus of the projection) for any generic projection of  $X$  to a plane. In Proposition 3.3 we show that the local bilipschitz constant of such a plane projection is bounded outside of a “very thin neighborhood” of the polar curves.

A thick-thin decomposition exists also for higher-dimensional germs, and we conjecture with Alberto Verjovsky that it can be made canonical. However, the

analogy with the Margulis thick-thin decomposition is no longer valid and the strong connection with complex geometry less clear, so it is also not yet clear how to get the full bilipschitz classification. The point is that topology in dimensions 5 and above is much more flabby. It is the rigidity of topology in dimension 3 and the nontriviality of fundamental groups in this dimension which enables the strong results for complex surfaces.

**Acknowledgments.** We are grateful to Jawad Snoussi, Don O'Shea, Guillaume Valette, and Alberto Verjovsky for useful conversations. In particular, Snoussi's paper [34] was very helpful to clarify some issues as we did this research. Neumann was supported by NSF grant DMS-0083097. Birbrair was supported by CNPq grants 201056/2010-0 and 300575/2010-6. We are also grateful for the hospitality/support of the following institutions: Jagiellonian University (B), Columbia University (B,P), Institut de Mathématiques de Luminy, Université de la Méditerranée, Instituto do Milénio (N), IAS Princeton, Universidad Federal de Ceara, CIRM petit groupe de travail (B,N,P).

## 2. CONSTRUCTION OF THE THICK-THIN DECOMPOSITION

To give the technical construction of the thick-thin decomposition for a normal complex surface germ  $(X, 0)$  we will need a suitably adapted resolution of  $(X, 0)$ .

Let  $\pi: (\tilde{X}, E) \rightarrow (X, 0)$  be the minimal resolution with the following properties:

- (1) It is a good resolution, i.e., the exceptional divisors are smooth and meet transversally, at most two at a time.
- (2) It resolves a generic pencil of hyperplane sections, i.e., the strict transforms of generic members of the pencil are disjoint. An exceptional curve intersecting the strict transforms of the generic members of the pencil will be called an  $\mathcal{L}$ -curve.
- (3) No  $\mathcal{L}$ -curve contains a basepoint of a system of polar curves of generic projections to  $\mathbb{C}^2$ .

This is achieved by starting with a minimal good resolution, then blowing up to resolve any basepoints of the family of hyperplane sections, and finally blowing up on  $\mathcal{L}$ -curves any basepoints of the family of polars. The last operation only creates strings of rational curves attached to  $\mathcal{L}$ -curves.

If two  $\mathcal{L}$ -curves intersected before the final operation, then the last operation above blows up the intersection point exactly once (see Lemma 3.10). In particular, two  $\mathcal{L}$ -curves cannot intersect in our resolution.

Let  $\Gamma$  be the resolution graph of the above resolution. A vertex of  $\Gamma$  is called a *node* if it has degree  $\geq 3$  or represents a curve of genus  $> 0$  or represents an  $\mathcal{L}$ -curve. If a node represents an  $\mathcal{L}$ -curve it is called an  $\mathcal{L}$ -node, otherwise a  $\mathcal{T}$ -node. By the previous paragraph,  $\mathcal{L}$ -nodes cannot be adjacent to each other.

The components of the result of removing the  $\mathcal{L}$ -nodes and adjacent edges from  $\Gamma$  are called the *Tjurina components* of  $\Gamma$  (following [35, Definition III.3.1]), so  $\mathcal{T}$ -nodes are precisely the nodes of  $\Gamma$  that are in Tjurina components.

A *string* is a connected subgraph of  $\Gamma$  containing no nodes. A *bamboo* is a string ending in a vertex of valence 1.

For each exceptional curve  $E_\nu$  in  $E$  let  $N(E_\nu)$  be a small closed tubular neighborhood. For any subgraph  $\Gamma'$  of  $\Gamma$  define (see Fig. 2):

$$N(\Gamma') := \bigcup_{\nu \in \Gamma'} N(E_\nu) \quad \text{and} \quad \mathcal{N}(\Gamma') := \overline{N(\Gamma)} \setminus \bigcup_{\nu \notin \Gamma'} N(E_\nu).$$

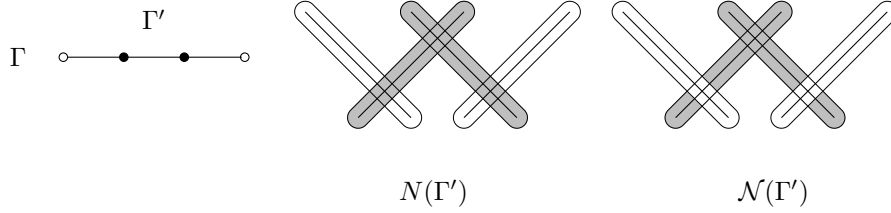


FIGURE 2.  $N(\Gamma')$  and  $\mathcal{N}(\Gamma')$  for the  $A_4$  singularity

In the Introduction we used standard  $\epsilon$ -balls to state our results, but in practice it is often more convenient to work with a different family of Milnor balls. For example, one can use, as in Milnor [29], the ball of radius  $\epsilon$  at the origin, or the balls with corners introduced by Kähler [17], Durfee [8] and others. In our proofs it will be convenient to use balls with corners, but it is a technicality to deduce the results for round Milnor balls. We will define the specific family of balls we use in Section 4. We denote it again by  $B_\epsilon$ ,  $0 < \epsilon \leq \epsilon_0$  and put  $S_\epsilon := \partial B_\epsilon$ .

**Definition 2.1** (Thick-thin decomposition). Assume  $\epsilon_0$  is sufficiently small that  $\pi^{-1}(X \cap B_{\epsilon_0})$  is included in  $N(\Gamma)$ . For each Tjurina component  $\Gamma_j$  which is not a bamboo define

$$Z_j := \pi(\mathcal{N}(\Gamma_j)) \cap B_{\epsilon_0}.$$

Let  $U_1, \dots, U_s$  be the closures of the connected components of  $\pi^{-1}(B_{\epsilon_0}) \setminus \bigcup_1^r \mathcal{N}(\Gamma_j)$  and denote

$$Y_i := \pi(U_i).$$

Notice that  $Y_i$  is  $\pi(N(\Gamma_\nu))$  where  $\Gamma_\nu$  consists of an  $\mathcal{L}$ -node  $\nu$  and any attached bamboos. So the  $Y_i$  are in one-one correspondence with the  $\mathcal{L}$ -nodes.

The  $Y_i$  are the *thick pieces* and the  $Z_j$  are the *thin pieces*.

By construction, the decomposition  $(X, 0) = \bigcup (Z_j, 0) \cup \bigcup (Y_i, 0)$  satisfies items (2) and (3) of Definition 1.4 and items (1) and (2) of Theorem 1.6. Item (3) of Theorem 1.6 and the thinness of the  $Z_j$  are proved in Section 5. The thickness of  $Y_i$  is proved in Section 6.

### 3. POLAR CURVES

Let  $(X, 0) \subset (\mathbb{C}^n, 0)$  be a normal surface germ and  $\ell: \mathbb{C}^n \rightarrow \mathbb{C}^2$  a linear projection. The *polar curve*  $\Pi = \Pi_\ell$  is the set of singular points of  $\ell|_X$ . In this section we prove two independent results about such polar curves which will be needed in the sequel.

We first explain what it means for  $\ell$  to be generic for  $X$ . Let  $\pi: (\tilde{X}, E) \rightarrow (X, 0)$  be our resolution and  $\Pi^* \subset \tilde{X}$  the strict transform of  $\Pi$  (also called the polar). As we vary the projection  $\ell$  we get a linear family  $\Pi_\ell^*$  of polars, and if necessary we

blow up further until this family has no basepoint. We will use this resolution for the rest of this section.

**Definition 3.1.** The linear projection  $\ell: \mathbb{C}^n \rightarrow \mathbb{C}^2$  is *generic* for  $X$  if the intersection of  $\Pi^*$  with  $E$  is generic in the above family. Moreover, the discriminant curve  $\Delta = \ell(\Pi)$  should be reduced; this means any  $p \in \Delta \setminus \{0\}$  has a neighbourhood  $U$  in  $\mathbb{C}^2$  such that one component of  $\ell|_X^{-1}(U)$  maps by a two-fold branched cover to  $U$  and the other components map bijectively. The fact that this is generic among linear projections  $\mathbb{C}^2 \rightarrow \mathbb{C}$  is explained, for example, in the introduction of [6].

The following improves Theorem 6.9 of Snoussi [34].

**Proposition 3.2.** *Let  $\Gamma_j$  be a Tjurina component of  $\Gamma$  and  $E^{(j)}$  the union of the  $E_\nu$  with  $\nu \in \Gamma_j$ . Then the strict transform of the polar curve of any linear projection to  $\mathbb{C}^2$  intersects  $E^{(j)}$ .*

*Proof.* The linear projection  $\ell$  is a finite covering ramified along its polar curve  $\Pi$ . Consider the resolution  $\pi: \tilde{X} \rightarrow X$ . We can choose  $N = N(\Gamma_j) \subset \tilde{X}$  so that it is a connected component of the closure of  $(\ell \circ \pi)^{-1}(C)$ , where  $C$  is the intersection of  $D_\epsilon^4 \setminus \{0\}$  with a conical neighborhood of a line in  $\mathbb{C}^2$ . If the strict transform by  $\pi$  of the polar curve of  $\ell$  does not intersect  $E^{(j)}$  then (after possibly shrinking  $N$  if necessary) it will be disjoint from  $N$ , so the restriction of  $\ell$  to  $\pi(N) \setminus \{0\}$  is a regular cover of  $C \setminus \{0\}$ . So the restriction to the link  $T := \pi(N) \cap S_\epsilon$  of  $\pi(N)$  is a covering of a solid torus. So  $T$  itself is a solid torus. Since  $T$  is obtained by plumbing according to  $\Gamma_j$ , this implies that  $\Gamma_j$  must be a bamboo. The meridian of  $T$ , which is null-homotopic in  $T$ , maps to a curve homotopic to  $d$  times the core of the image torus, where  $d > 0$  is the absolute value of the determinant associated with  $\Gamma_j$ . This is a contradiction.  $\square$

Let  $K: X \setminus \{0\} \rightarrow \mathbb{R} \cup \{\infty\}$  be the local bilipschitz constant for the linear projection  $\ell|_X$ . It is infinite on the polar curve and at a point  $p \in X \setminus \Pi$  it is the reciprocal of the shortest length among images of unit vectors in  $T_p X$  under the projection  $d\ell: T_p X \rightarrow \mathbb{C}^2$ .

**Proposition 3.3** (Very Thin Zone Lemma). *Assume the linear projection  $\ell$  is generic for  $X$ . Given any neighbourhood  $U$  of  $\Pi^* \cap \pi^{-1}(B_\epsilon)$  in  $\tilde{X} \cap \pi^{-1}(B_\epsilon)$ , for  $K_0$  sufficiently large the set*

$$B_{K_0} := \{p \in X \cap (B_\epsilon \setminus 0) : K(p) \geq K_0\},$$

*is a subset of  $\pi(U)$ .*

*Proof.* We choose coordinates in  $\mathbb{C}^n$  so that every orthogonal projection to a coordinate plane is generic for  $X$  and our projection  $\ell$  is the projection to the  $(z_1, z_2)$ -plane. We first consider the case that  $X$  is a complete intersection, given by equations

$$f_i(z_1, \dots, z_n) = 0 \quad i = 1, \dots, n-2.$$

Write

$$(3) \quad J := \left( \frac{\partial f_i}{\partial z_j} \right)_{\substack{i=1, \dots, n-2 \\ j=1, \dots, n}},$$



the Jacobian matrix of  $f = (f_1, \dots, f_{n-2})^t: \mathbb{C}^n \rightarrow \mathbb{C}^{n-2}$ , and write

$$(4) \quad J_0 := \begin{pmatrix} \frac{\partial f_i}{\partial z_j} \end{pmatrix}_{\substack{i=1, \dots, n-2 \\ j=3, \dots, n}}.$$

**Lemma 3.4.** *The equation  $\det J_0 = 0$  on  $X$  is the equation of the polar curve  $\Pi = \Pi_\ell$ .*

*Proof.* At a point  $p \in X$  the equation  $\det J_0 = 0$  is equivalent to

$$\det \begin{pmatrix} 1 & 0 & \dots & 0 & 0 \\ 0 & 1 & \dots & 0 & 0 \\ & & J(p) & & \end{pmatrix} = 0$$

which expresses the fact that the rows of this matrix do not span  $\mathbb{C}^n$ , or equivalently, that the orthogonal complement of the last  $n-2$  rows, which is  $T_p X$ , intersects non-trivially the orthogonal complement of the first two rows, which is the kernel of the projection  $\ell$ .  $\square$

A vector  $(a_1, \dots, a_n)^t \in \mathbb{C}^n$  is in  $T_p X$  if and only if

$$(5) \quad h_i := \sum_{j=1}^n a_j \overline{\frac{\partial f_i}{\partial z_j}}(p) = 0 \quad \text{for } i = 1, \dots, n-2.$$

Moreover, the vector has unit length if and only if

$$(6) \quad h := |a_1|^2 + \dots + |a_n|^2 - 1 = 0.$$

So we wish to minimize  $L := |a_1|^2 + |a_2|^2$  subject to the constraints (5) and (6);  $K(p)$  is then  $\frac{1}{\sqrt{L}}$ . Using Lagrange multipliers and differentiating  $L - \lambda h - \sum_{i=1}^{n-2} \lambda_i h_i$  with respect to  $a_1, \dots, a_n$  leads to the equation

$$(7) \quad \begin{pmatrix} \overline{a_1} \\ \overline{a_2} \\ 0 \\ \vdots \\ 0 \end{pmatrix} = \lambda \begin{pmatrix} \overline{a_1} \\ \vdots \\ \overline{a_{n-2}} \\ \overline{a_{n-1}} \\ \overline{a_n} \end{pmatrix} + \overline{J(p)}^t \begin{pmatrix} \lambda_1 \\ \vdots \\ \lambda_{n-2} \end{pmatrix}$$

with  $\lambda, \lambda_1, \dots, \lambda_{n-2} \in \mathbb{R}$ . Multiplying this matrix equation from the left by  $(a_1, \dots, a_n)$  gives  $|a_1|^2 + |a_2|^2 = \lambda(|a_1|^2 + \dots + |a_n|^2)$  by (5), hence  $|a_1|^2 + |a_2|^2 = \lambda$  by (6). So after solving the simultaneous equations (5), (6) and (7) for the  $a_j$ 's, the  $\lambda_i$ 's and  $\lambda$ , the resulting  $\lambda$  is the minimal  $L$  we seek.

We can rewrite equation (7) as

$$(8) \quad \begin{pmatrix} \overline{a_1} \\ \overline{a_2} \\ \overline{a_3} \\ \vdots \\ \overline{a_n} \end{pmatrix} = \begin{pmatrix} \lambda - 1 & & & & 0 \\ & \lambda - 1 & & & \\ & & \lambda & & \\ & & & \ddots & \\ 0 & & & & \lambda \end{pmatrix}^{-1} \overline{J(p)}^t \begin{pmatrix} \lambda_1 \\ \vdots \\ \lambda_{n-2} \end{pmatrix}$$

and left-multiplying this by  $\lambda(\lambda - 1)J(p)$  gives

$$(9) \quad 0 = J(p) \begin{pmatrix} -\lambda & & & 0 \\ & -\lambda & & \\ & & 1 - \lambda & \\ & & & \ddots \\ 0 & & & & 1 - \lambda \end{pmatrix} \overline{J(p)}^t \begin{pmatrix} \lambda_1 \\ \vdots \\ \lambda_{n-2} \end{pmatrix}$$

which can be rewritten

$$(10) \quad 0 = (J_0(p)\overline{J_0(p)}^t - \lambda J(p)\overline{J(p)}^t) \begin{pmatrix} \lambda_1 \\ \vdots \\ \lambda_{n-2} \end{pmatrix}.$$

Now if  $T_p X$  is the  $(z_1, z_2)$  plane then  $\lambda = 1$ , but otherwise  $\lambda$  must be less than 1 and then (7) implies that  $\lambda_1, \dots, \lambda_{n-2}$  cannot all be zero, so the linear equation (10) has a nontrivial solution. It follows that for any  $p$

$$(11) \quad \det(J_0(p)\overline{J_0(p)}^t - \lambda J(p)\overline{J(p)}^t) = 0.$$

This is a polynomial of degree  $n-2$  in  $\lambda$  with highest coefficient  $(-1)^{n-2} \det(J(p)\overline{J(p)}^t)$  and constant term  $\det(J_0(p)\overline{J_0(p)}^t)$ , so the product of its zeros is

$$(12) \quad M(p) := \frac{\det(J_0(p)\overline{J_0(p)}^t)}{\det(J(p)\overline{J(p)}^t)}.$$

**Lemma 3.5.** *The map  $M \circ \pi$  is well defined and real analytic on our resolution  $\tilde{X}$  and vanishes only on  $\Pi^*$ .*

*Proof.* The following linear algebra lemma is easily verified

**Lemma 3.6.** *If  $A$  is a  $k \times n$  matrix with  $k \leq n$  then  $\det(A\overline{A}^t) = \sum_{A'} |\det A'|^2$ , sum over all  $k \times k$  minors of  $A$ .  $\square$*

Applying this lemma to  $M(p)$  shows that it is the ratio

$$(13) \quad M(p) = \frac{|\det J_{[1,2]}(p)|^2}{\sum_{1 \leq i < j \leq n} |\det J_{[i,j]}(p)|^2}$$

where  $J_{[i,j]}$  is the minor of  $J$  obtained by deleting columns  $i$  and  $j$  (so  $J_{[1,2]} = J_0$ ). By Lemma 3.4,  $\det(J_{[i,j]}) = 0$  is the equation of the polar curve for the projection to the  $(z_i, z_j)$ -plane, and by our genericity assumption, the order of vanishing of  $\det J_{[i,j]}$  on any exceptional curve of our resolution does not depend on  $(i, j)$ . Thus the denominator of (13) vanishes to the same order as the numerator, proving Lemma 3.5.  $\square$

Since  $M(p)$  is a product of zeros of (11), one of which is  $\lambda = \lambda(p)$ , it follows that  $\lambda \circ \pi$  vanishes only on  $\Pi^*$ , so  $K \circ \pi = \frac{1}{\sqrt{\lambda \circ \pi}}$  is defined and continuous off  $\Pi^*$ . This completes the proof of Proposition 3.3 in the case that  $X$  is a complete intersection.

If  $X$  is not a complete intersection, let  $f_1 = \dots = f_r = 0$  be a minimal set of defining equations. The matrix  $(\frac{\partial f_i}{\partial z_j})$  has rank  $n - 2$  at any point  $p$  of  $X \setminus \{0\}$  so in a neighborhood of each point we can choose  $n - 2$  of the  $f_i$ 's and argue as before. This collection of  $f_i$ 's will in general give a smaller rank on some curve in  $X$ . For each  $(n - 2)$ -element subset  $S$  of  $\{1, \dots, r\}$  let  $C_S$  be the strict transform in

$\widetilde{X}$  of this curve. So long as not all these curves have a common intersection point on  $\widetilde{X} \setminus \Pi^*$  our previous argument applies, while if they do all have some common intersection points, such a point must lie on the exceptional divisor, and we can eliminate it by performing additional blow-ups at the point. This completes the proof of Proposition 3.3.  $\square$

Recall that the *discriminant curve*  $\Delta \subset \mathbb{C}^2$  is the image  $\ell(\Pi)$  of the polar curve  $\Pi$ . Let  $\delta$  be a component of  $\Delta$  and choose coordinates in  $\mathbb{C}^2$  so that  $\delta$  is tangent to the  $x$ -axis. The curve  $\delta$  admits a Puiseux series expansion of the form

$$y = \sum_{j \geq 1} a_j x^{p_j} \in \mathbb{C}\{x^{\frac{1}{N}}\}$$

Here  $1 < p_1 < p_2 < \dots$  are in  $\mathbb{Q}$  and the denominator  $\text{denom}(p_j)$  a divisor of  $N$  for each  $j$ .

Recall that a Puiseux exponent  $p_j$  is *characteristic* if the embedded topology of the plane curves  $y = \sum_{i=1}^{j-1} a_i x^{p_i}$  and  $y = \sum_{i=1}^j a_i x^{p_i}$  differ; equivalently  $\text{denom}(p_j)$  does not divide  $\text{lcm}_{i < j} \text{denom}(p_i)$ . We denote the characteristic exponents by  $p_{j_k}$  for  $k = 1, \dots, r$ .

With  $B_{K_0}$  as in Proposition 3.3, let  $N_{K_0}(\delta)$  denote the closure of the connected component of  $\ell(B_{K_0}) \setminus \{0\}$  which contains  $\delta \setminus \{0\}$ .

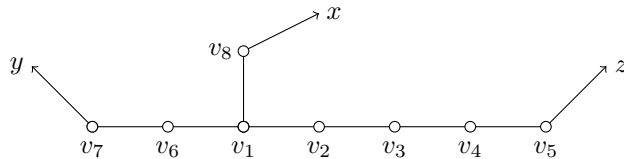
**Corollary 3.7.** *There exists  $s \geq p_{j_r}$  such that for any  $\alpha > 0$  there is  $K_0 \geq 1$  such that  $N_{K_0}(\delta)$  is contained in a set of the form*

$$\{(x, y) : \left| y - \sum_{j=1}^{j_r} a_j x^{p_j} \right| \leq \alpha |x|^s\}.$$

We shall prove this for  $s = p_{j_r}$ , but typically  $s$  can be chosen strictly greater. For example, as we show below, for the singularity  $X(2, 3, 5) = \{(x, y, z) \in \mathbb{C}^3 : x^2 + y^3 + z^5 = 0\}$  we have  $p_{j_r} = \frac{5}{3}$  and  $s$  can be chosen as  $\frac{10}{3}$ .

*Proof.* According to the Very Thin Zone Lemma 3.3,  $B_{K_0}$  is contained in a neighborhood  $A$  of the polar curve  $\Pi$  which is saturated by polar curves  $\Pi_t$  of a family of generic projections  $\ell_t$  indexed by  $t \in D^2$ , with  $\ell_0 = \ell$  and  $\Pi_0 = \Pi$ . The image  $\ell(A)$  is thus a neighborhood of  $\Delta$  saturated by images  $\ell(\Pi_t)$ . If  $\delta_t, t \in D^2$  is the family of components of  $\ell(\Pi_t)$  which saturates a neighborhood of  $\delta$  then the Puiseux series for  $\delta_t$  must agree up to at least the last characteristic term  $y^{q_{j_r}/p_{j_r}}$  with that of  $\delta$ , except that the coefficient of that last agreeing term could differ a small amount (bounded in terms of  $1/K_0$  and  $t$ ) from that for  $\delta$ .  $\square$

**Example 3.8.** Let  $(X, 0)$  be the  $E_8$  singularity with equation  $x^2 + y^3 + z^5 = 0$ . Its resolution graph, with all Euler weights  $-2$  and decorated with arrows corresponding to the strict transforms of the coordinate functions  $x, y$  and  $z$ , is:



We denote by  $C_j$  the exceptional curve corresponding to the vertex  $v_j$ . Then the total transform by  $\pi$  of the coordinate functions  $x, y$  and  $z$  are:

$$\begin{aligned}(x \circ \pi) &= 15C_1 + 12C_2 + 9C_3 + 6C_4 + 3C_5 + 10C_6 + 5C_7 + 8C_8 + x^* \\ (y \circ \pi) &= 10C_1 + 8C_2 + 6C_3 + 4C_4 + 2C_5 + 7C_6 + 4C_7 + 5C_8 + y^* \\ (z \circ \pi) &= 6C_1 + 5C_2 + 4C_3 + 3C_4 + 2C_5 + 4C_6 + 2C_7 + 3C_8 + z^*\end{aligned}$$

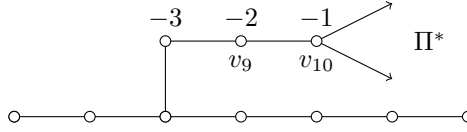
Set  $f(x, y, z) = x^2 + y^3 + z^5$ . The polar curve  $\Pi$  of a generic linear projection  $\ell: (X, 0) \rightarrow (\mathbb{C}^2, 0)$  has equation  $g = 0$  where  $g$  is a generic linear combination of the partial derivatives  $f_x = 2x$ ,  $f_y = 3y^2$  and  $f_z = 5z^4$ . The multiplicities of  $g$  are given by the minimum of the compact part of the three divisors

$$\begin{aligned}(f_x \circ \pi) &= 15C_1 + 12C_2 + 9C_3 + 6C_4 + 3C_5 + 10C_6 + 5C_7 + 8C_8 + f_x^* \\ (f_y \circ \pi) &= 20C_1 + 16C_2 + 12C_3 + 8C_4 + 4C_5 + 14C_6 + 8C_7 + 10C_8 + f_y^* \\ (f_z \circ \pi) &= 24C_1 + 20C_2 + 16C_3 + 12C_4 + 8C_5 + 16C_6 + 8C_7 + 12C_8 + f_z^*\end{aligned}$$

We then obtain that the total transform of  $g$  is equal to:

$$(g \circ \pi) = 15C_1 + 12C_2 + 9C_3 + 6C_4 + 3C_5 + 10C_6 + 5C_7 + 8C_8 + \Pi^*.$$

In particular,  $\Pi$  is resolved by  $\pi$  and its strict transform  $\Pi^*$  has just one component, which intersects  $C_8$ . Since the multiplicities  $m_8(f_x) = 8$ ,  $m_8(f_y) = 10$  and  $m_8(z) = 12$  along  $C_8$  are distinct, the pencil of polar curves of generic linear projections has a base point on  $C_8$ . One must blow-up twice to get an exceptional curve  $C_{10}$  along which  $m_{10}(f_x) = m_{10}(f_y)$ , which resolves the pencil. Then  $N_{K_0}(\delta)$  is the image by  $\pi$  of a neighbourhood of  $\Pi^*$  of the form  $D^2 \times \text{fibre}$  where  $D^2$  is a small disc neighbourhood of  $\Pi^* \cap C_{10}$  in  $C_{10}$ .



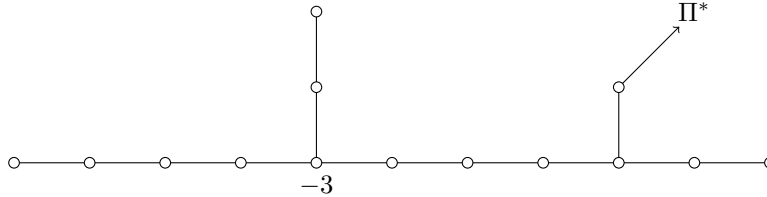
We now compute the maximal  $s$  in Corollary 3.7. Since the generic polar has equation  $x + ay^2 + bz^4 = 0$  with  $a, b \in \mathbb{C}$ , its image  $\Delta_{a,b}$  in  $\mathbb{C}^2$  under the projection  $\ell = (y, z)$  has equation

$$y^3 + a^2y^4 + 2aby^2z^4 + z^5 + b^2z^8 = 0$$

$\Delta_{0,0}$  is a generic polar with Puiseux expansion  $y = (-z)^{5/3}$ , while for  $(a, b) \neq (0, 0)$ , we get a Puiseux expansion of the form:  $y = (-z)^{5/3} + cz^{10/3} + \dots$

Thus any  $s$  with  $5/3 \leq s \leq 10/3$  realizes the condition of 3.7.

**Example 3.9.** Consider  $(X, 0)$  with equation  $z^2 + xy^{14} + (x^3 + y^5)^3 = 0$ . The dual graph of the minimal resolution  $\pi$  has two nodes, one of them with Euler class  $-3$ . All other vertices have Euler class  $-2$ . Similar computations show that  $\pi$  also resolves the polar  $\Pi$  and we get:



Denoting by  $C_1$  the exceptional curve such that  $C_1 \cap \Pi^* \neq \emptyset$ , we get  $m_1(f_x) \geq 124$ ,  $m_1(f_y) = 130$  and  $m_1(f_z) = 71$ . Then the pencil of polars admits a base point on  $C_1$  and one has to perform at least  $124 - 71 = 53$  blow-ups to resolve it. In this case one computes that the discriminant curve has two essential exponents,  $5/3$  and  $17/9$ , and one can choose any  $s$  with  $17/9 \leq s \leq 124/9$ .

The following lemma was promised in Section 2. Recall that the resolution  $\pi: \tilde{X} \rightarrow X$  which we use is obtained from a minimal good resolution by first blowing up base points of generic hyperplane sections and then blowing up base points on  $\mathcal{L}$ -curves of the family of generic polar curves. Before the final step there may be intersecting  $\mathcal{L}$ -curves.

**Lemma 3.10.** *If there are intersecting  $\mathcal{L}$ -curves as above then for any generic plane projection the strict transform of the polar has exactly one component through that common point and it intersects the two  $\mathcal{L}$ -curves transversally.*

*Proof.* Denote the two intersecting  $\mathcal{L}$ -curves  $E_\mu$  and  $E_\nu$  and choose coordinates  $(u, v)$  centered at the intersection such that  $E_\mu$  and  $E_\nu$  are locally given by  $u = 0$  and  $v = 0$  respectively. We assume our plane projection is given by  $\ell = (x, y): \mathbb{C}^n \rightarrow \mathbb{C}^2$ , so  $x$  and  $y$  are generic linear forms. Then without loss of generality  $x = u^m v^n$  in our local coordinates, and  $y = u^m v^n (a + bu + cv + g(u, v))$  with  $a \neq 0$  and  $g$  of order  $\geq 2$ . The fact that  $E_\mu$  and  $E_\nu$  are  $\mathcal{L}$ -curves means that  $c \neq 0$  and  $b \neq 0$  respectively. The polar is given by vanishing of the Jacobian determinant  $\det \frac{\partial(x, y)}{\partial(u, v)} = u^{2m-1} v^{2n-1} (mcv - nbu + mvg_v - nug_u)$ . Modulo terms of order  $\geq 2$  this vanishing is the equation  $v = \frac{nb}{mc} u$ , proving the lemma.  $\square$

#### 4. MILNOR BALLS

From now on we assume our coordinates  $(z_1, \dots, z_n)$  in  $\mathbb{C}^n$  are chosen so that  $z_1$  and  $z_2$  are generic linear forms and  $\ell := (z_1, z_2): X \rightarrow \mathbb{C}^2$  is a generic linear projection. In this section we denote by  $B_\epsilon^{2n}$  the standard round ball in  $\mathbb{C}^n$  of radius  $\epsilon$  and  $S_\epsilon^{2n-1}$  its boundary.

The family of Milnor balls we use in the sequel consists of standard “Milnor tubes” associated with the Milnor-Lê fibration for the map  $\zeta := z_1|_X: X \rightarrow \mathbb{C}$ . Namely, for some sufficiently small  $\epsilon_0$  and some  $R > 0$  we define for  $\epsilon \leq \epsilon_0$ :

$$B_\epsilon := \{(z_1, \dots, z_n) : |z_1| \leq \epsilon, |(z_1, \dots, z_n)| \leq R\epsilon\} \quad \text{and} \quad S_\epsilon = \partial B_\epsilon,$$

where  $\epsilon_0$  and  $R$  are chosen so that for  $\epsilon \leq \epsilon_0$ :

- (1)  $\zeta^{-1}(t)$  intersects  $S_{R\epsilon}^{2n-1}$  transversally for  $|t| \leq \epsilon$ ;
- (2) the polar curves for the projection  $\ell = (z_1, z_2)$  meet  $S_\epsilon$  in the part  $|z_1| = \epsilon$ .

We claim that such  $\epsilon_0$  and  $R$  exist.

We can clearly achieve (2) by choosing  $R$  sufficiently large, since the polar curves lie close to exceptional tangent directions, which are transverse to the hyperplane  $z_1 = 0$  by genericity of  $z_1$ .

To see that we can achieve (1) note that for  $p \in X$  and  $t = \zeta(p)$  the sphere  $S_{|p|}^{2n-1}$  is transverse to  $\zeta^{-1}(t)$  at the point  $p$  if and only if the intersection  $T_p X \cap \{z_1 = 0\}$  is not orthogonal to the direction  $\frac{\vec{p}}{|p|}$  (considering  $T_p X$  as a subspace of  $\mathbb{C}^n$ ). We will say briefly that condition  $T(p)$  holds.

First choose  $r > 0$  so that the round balls  $B_\epsilon^{2n}$  for  $\epsilon \leq r$  are a family of Milnor balls for the pair  $(X, \zeta^{-1}(0))$ . Then condition  $T(p)$  holds for all points of  $\zeta^{-1}(0) \cap$

$B_r^{2n}$ . We must show there exists  $R > 0$  so that  $T(p)$  holds for all  $p$  in

$$C_R := \{p \in X : R|\zeta(p)| \leq |p| \leq r\},$$

since then  $R$  and  $\epsilon_0 := \frac{r}{R}$  do what is required. Since  $C_\infty = \zeta^{-1}(0) \cap B_r^{2n}$ , we know  $T(p)$  holds for  $p \in C_\infty$ , and as we decrease  $R$  through sufficiently large values the closure of the set of pairs  $(T_p X, \frac{\tilde{p}}{|p|})$  for  $p \in C_R$  (as a subset of  $G_2^n(\mathbb{C}) \times S^{2n-1}$  where  $G_2^n(\mathbb{C})$  is the grassmanian) is a compact set which increases continuously, since otherwise the tangent line of  $C_\infty$  at 0 would be an exceptional tangent. It follows that for sufficiently large  $R$  condition  $T(p)$  is satisfied for all  $p \in C_R$ .

## 5. THE THIN PIECES

In this section we prove the thinness of the pieces  $Z_j$  defined section 2. We start with a proof of Proposition 1.3:

*Proof.* Without loss of generality  $Z$  is closed. The tangent cone  $TZ$  of  $Z$  is the cone over the Hausdorff limit  $\lim_{\epsilon \rightarrow 0} (\frac{1}{\epsilon} Z \cap S_1)$ . Thus for any  $C > 0$  the function  $f: \epsilon \mapsto d(Z \cap S_\epsilon, TZ \cap S_\epsilon)$  satisfies  $f(\epsilon) < C\epsilon$  for  $\epsilon$  sufficiently small ( $d$  denotes the Hausdorff distance). Since  $f$  is semi-algebraic, there is a  $c > 0$  and Lojasiewicz exponent  $q > 1$  such that  $f(\epsilon) \leq c\epsilon^q$  for all  $\epsilon$  sufficiently small. This proves the proposition.  $\square$

**Proposition 5.1. 1.** *For each  $j$  there is an exceptional tangent line  $L_j$  at 0 of  $(X, 0)$  and constants  $c_j > 0$  and  $q_j > 1$  such that  $Z_j \cap B_\epsilon$  is contained in an  $(c_j \epsilon^{q_j})$ -neighborhood of the line  $L_j$ .*

**2.** *In fact, the restriction  $\zeta_j: Z_j \setminus \{0\} \rightarrow D_\epsilon^2 \setminus \{0\}$  of  $z_1$  is a locally trivial fibration such that each fiber  $\zeta_j^{-1}(t)$  lies in an  $(c_j \epsilon^{q_j})$ -neighborhood of the point  $L_j \cap \{z_1 = t\}$  (we call these fibers the Milnor fibers of  $Z_j$ ).*

**3.** *There is a vector field  $v_j$  on  $Z_j \setminus \{0\}$  which lifts by  $\zeta_j$  the inward radial unit vector field on  $\mathbb{C} \setminus \{0\}$  and has the property that any two integral curves for  $v_j$  starting at points of  $Z_j$  with the same  $z_1$  coordinate approach each other faster than linearly. In particular, the flow along this vector field takes Milnor fibers to Milnor fibers while shrinking them faster than linearly.*

Note that it follows from part 1 of this proposition that, with our choice of Milnor balls as in section 4, the link  $Z_j^{(\epsilon)} = Z_j \cap S_\epsilon$  is included in the  $|z_1| = \epsilon$  part of  $S_\epsilon$ .

We need the following lemma. For any  $h \in \mathcal{O}_{X,0}$  denote  $\tilde{h} := h \circ \pi: \tilde{X} \rightarrow \mathbb{C}$  and denote by  $m_\nu(h)$  the multiplicity of  $\tilde{h}$  along the exceptional curve  $E_\nu$ .

**Lemma 5.2.** *Let  $h_1 = \zeta = z_1|_X$ . For any Tjurina component there exist functions  $h_2, \dots, h_m \in \mathcal{O}_{X,0}$  such that  $h_1, \dots, h_m$  generate  $\mathcal{O}_{X,0}$ , and such that for any vertex  $\nu$  of the Tjurina component we have  $m_\nu(h_i) > m_\nu(h_1)$  for  $i > 1$ .*

*Proof.* Take any functions  $g_2, \dots, g_m \in \mathcal{O}_{X,0}$  such that  $h_1$  and  $g_2, \dots, g_m$  generate  $\mathcal{O}_{X,0}$ . Choose a vertex  $\nu$  of the Tjurina component. By choice of  $z_1$  we know  $m_\nu(h_1) \leq m_\nu(g_i)$  for all  $i > 1$ . Choose a point  $p$  on  $E_\nu$  distinct from the intersections with other exceptional curves and the strict transform of  $g_i^{-1}(0)$ . Then  $\tilde{h}_1$  and  $\tilde{g}_i$  are given in local coordinates  $(u, v)$  centered at  $p$  by  $\tilde{h}_1 = u^{m_\nu(h_1)}(a_1 + \alpha_1(u, v))$  and  $\tilde{g}_i = u^{m_\nu(h_1)}(a_i + \alpha_i(u, v))$  where  $a_1 \neq 0$  and  $\alpha_i(0, 0) = \alpha_i(0, 0) = 0$ . Let  $h_i := g_i - \frac{a_i}{a_1} h_1$  for  $i = 2, \dots, m$ . Then  $h_1, \dots, h_m$  generate  $\mathcal{O}_{X,0}$ . If the multiplicity of  $\tilde{h}_i$  on  $E_\nu$  is  $m_\nu(h_1)$  then the strict transform of  $h_i^{-1}(0)$  passes through  $p$ .

We can choose  $p$  so this is not so, since otherwise the node  $\nu$  would be an  $\mathcal{L}$ -node. Thus  $m_\nu(h_i) > m_\nu(h_1)$ .

We now claim that  $m_\mu(h_i) > m_\mu(h_1)$  for  $i > 1$  for any vertex  $\mu$  of the Tjurina component adjacent to  $\nu$  (it then follows inductively for every vertex of the Tjurina component). So let  $\mu$  be such a vertex and assume that  $m_\mu(h_i) = m_\mu(h_1)$ . Consider the meromorphic function  $\tilde{h}_1/\tilde{h}_i$  on  $E_\mu$ . It takes finite values almost everywhere and has a pole at  $E_\mu \cap E_\nu$  so it must have a zero at some point of  $E_\mu$ . This cannot happen since  $m_{\nu'}(h_1) \leq m_{\nu'}(h_i)$  for any  $\nu'$  and the strict transform of the zero set of  $h_1$  only intersects the  $\mathcal{L}$ -nodes ( $h_1$  is the generic linear form).  $\square$

*Proof of Proposition 5.1.* Let  $h_1, \dots, h_m$  be as in Lemma 5.2 and let

$$q_j := \min \left\{ 2, \frac{m_\nu(h_i)}{m_\nu(h_1)} : \nu \in \Gamma_j, i > 1 \right\}.$$

For each  $k = 2, \dots, n$  one has

$$z_k|_X = \lambda_j h_1 + \beta_k$$

with  $\lambda_k \in \mathbb{C}$  and  $\beta_k \in (h_1^2, h_2, \dots, h_m)$ .

Let  $L_j$  be the line in  $\mathbb{C}^n$  parametrized by  $(t, \lambda_2 t, \dots, \lambda_n t)$ ,  $t \in \mathbb{C}$ .

Consider local coordinates  $(u, v)$  in a compact neighborhood of a point of  $E_\nu \setminus \bigcup_{\mu \neq \nu} E_\mu$  in which  $\tilde{\beta}_i = u^{m_\nu(\beta_i)}(a_i + \alpha_i(u, v))$  with  $a_i \neq 0$  and  $\alpha_i$  holomorphic. In this neighborhood  $|\tilde{z}_i - \lambda_i \tilde{z}_1| = O(|\tilde{z}_1|^{m_\nu(\beta_i)/m_\nu(h_1)}) = O(|\tilde{z}_1|^{q_j})$ .

In a neighborhood of a point  $E_\nu \cap E_\mu$  of intersection of two exceptional curves of the Tjurina component we have local coordinates  $u, v$  such that  $\tilde{h}_1 = u^{m_\mu(h_1)}v^{m_\nu(h_1)}$  and  $\tilde{\beta}_i = u^{m_\mu(\beta_i)}v^{m_\nu(\beta_i)}(a_i + \alpha_i(u, v))$  with  $a_i \neq 0$  and  $\alpha_i$  holomorphic. In this neighborhood we again have  $|\tilde{z}_i - \lambda_i \tilde{z}_1| = O(|\tilde{z}_1|^{q_j})$ .

By compactness of  $\mathcal{N}(\Gamma_j)$  the estimate  $|\tilde{z}_i - \lambda_i \tilde{z}_1| = O(|\tilde{z}_1|^{q_j})$  holds on all of  $\mathcal{N}(\Gamma_j)$ . Thus, if we define  $f_j: Z_j = \pi(\mathcal{N}(\Gamma_j)) \rightarrow \mathbb{C}^n$  by  $f_j(p) := z_1(p)(1, \lambda_2, \dots, \lambda_n)$ , we have shown that  $|p - f_j(p)| = O(z_1(p)^{q_j})$ . In particular, for  $p \in \mathcal{N}(\Gamma_j)$  the distance of  $\pi(p)$  from 0 is  $O(|z_1(p)|)$ , and therefore  $Z_j \cap B_\epsilon$  is contained in an  $(c_j \epsilon^{q_j})$ -neighborhood of the line  $L_j$  for some  $c_j > 0$ .

In particular, we see that  $Z_j$  is thin, and tangent to the line  $L_j$ . Thus each limit of tangent hyperplanes at a sequence of points converging to 0 in  $Z_j \setminus \{0\}$  contains  $L_j$ . We will show there exist infinitely many such limits, which, by definition, means that  $L_j$  is an exceptional tangent line (this is a short proof of one of the two implications of Proposition 6.3 of Snoussi [34], see also Proposition 2.2.1 of [23]). Indeed, for any generic  $(n-2)$ -plane  $H$  let  $\ell_H: \mathbb{C}^n \rightarrow \mathbb{C}^2$  be the projection with kernel  $H$ . By Proposition 3.2 the strict transform  $\Pi^*$  of the polar  $\Pi$  of  $\ell_H|_X$  intersects  $\bigcup_{\nu \in \Gamma_j} E_\nu$ . Let  $C$  be a branch of  $\Pi^*$  which intersects  $\bigcup_{\nu \in \Gamma_j} E_\nu$ . Then at each  $p \in C$  the tangent plane to  $X$  at  $p$  intersects  $H$  non-trivially, so the limit of these planes as  $p \rightarrow 0$  in  $C$  is a plane containing  $L_j$  which intersects  $H$  non-trivially. By varying  $H$  we see that there are infinitely many such limits along sequences of points approaching 0 along curves tangent to  $L_j$ , as desired.

Part 2 of Proposition 5.1 is just the observation that  $\zeta_j$  is the restriction to  $Z_j \setminus \{0\}$  of the Milnor-Lê fibration for  $z_1: X \rightarrow \mathbb{C}$ .

For part 3 we will use local coordinates as above to construct the desired vector field locally in  $\pi^{-1}(Z_j \setminus \{0\})$ ; it can then be glued together by a standard partition of unity argument. Specifically, in a neighborhood of a point  $p$  of  $E_\nu \setminus \bigcup_{\mu \neq \nu} E_\mu$ ,

using coordinates  $(u = r_u e^{i\theta_u}, v = r_v e^{i\theta_v})$  with  $\tilde{h}_1 = u^{m_\nu(h_1)}$ , the vector field

$$\left( \frac{1}{mr_u^{m-1}} \frac{\partial}{\partial r_u}, 0 \right)$$

with  $m = m_\nu(h_1)$  works, while in a neighborhood of a point  $E_\nu \cap E_\mu$ , using coordinates with  $\tilde{h}_1 = u^{m_\nu(h_1)} v^{m_\mu(h_1)}$ , the vector field

$$\left( \frac{1}{mr_u^{m-1} r_v^{m'}} \frac{\partial}{\partial r_u}, \frac{1}{m' r_u^m r_v^{m'-1}} \frac{\partial}{\partial r_v} \right)$$

with  $m = m_\nu(h_1)$  and  $m' = m_\mu(h_1)$  works.  $\square$

## 6. THE THICK PIECES

As before,  $\ell = (z_1, z_2): B_{\epsilon_0} \rightarrow (\mathbb{C}^2, 0)$  is a generic linear projection to  $\mathbb{C}^2$  and  $\Pi$  the polar curve for this projection. By choice of the resolution  $\pi$ , the strict transform  $\Pi^*$  of the polar curve meets  $\mathcal{L}$ -curves only at smooth points of  $E$ . After performing additional blowups at such points, we may assume that  $\Pi^*$  does not meet any  $\mathcal{L}$ -curve. Notice that such sequences of blow-ups only create bamboos attached to the  $\mathcal{L}$ -nodes. We work with this resolution graph throughout this section; we still call it  $\Gamma$ .

Recall that a thick piece is a region of the form  $Y = \pi(N(\Gamma_\nu))$ , where  $\Gamma_\nu$  consists of an  $\mathcal{L}$ -node  $\nu$  and any attached bamboos. The thickness of  $Y$  follows from the following Lemma, of which part (3), the conicalness of the pieces coming from bamboos, is the most difficult. Once we have the lemma, the conicalness of the union of the conical piece  $\pi(\mathcal{N}(\nu))$  with the conical pieces coming from the bamboos follows from [37, Corollary 0.2] and part (2) of the lemma (or rather, its proof) then completes the proof that  $Y$  is thick.

**Lemma 6.1.** *For any  $\mathcal{L}$ -node  $\nu$  we have that*

- (1)  $\pi(\mathcal{N}(\nu))$  is metrically conical;
- (2)  $\pi(N(E_\nu))$  is thick;
- (3) for any bamboo  $\Gamma'$  attached to  $\nu$  we have that  $\pi(N(\Gamma'))$  is conical.

*Proof of part (1).* From now on we work only inside of a Milnor ball  $B_{\epsilon_0}$  as defined in Section 4 and  $X$  now means  $X \cap B_{\epsilon_0}$ .

Denote by  $\Delta = \Delta_1 \cup \dots \cup \Delta_k \subset \mathbb{C}^2$  the decomposition of the discriminant curve  $\Delta$  for  $\ell$  into its irreducible components. By genericity, we can assume the tangent lines in  $\mathbb{C}^2$  to the  $\Delta_i$  are of the form  $z_2 = b_i z_1$ . Denote

$$V_i := \{(z_1, z_2) \in \mathbb{C}^2 : |z_1| \leq \epsilon_0, |z_2 - b_i z_1| \leq \eta |z_1|\},$$

where we choose  $\eta$  small enough that  $V_i \cap V_j = \{0\}$  if  $b_i \neq b_j$  and  $\epsilon_0$  small enough that  $\Delta_i \cap \{(z_1, z_2) : |z_1| \leq \epsilon_0\} \subseteq V_i$ . Notice that if two  $\Delta_i$ 's are tangent then the corresponding  $V_i$ 's are the same.

Let  $W_{i1}, \dots, W_{ij_i}$  be the closure of the connected components of  $X \cap \ell^{-1}(V_i \setminus \{0\})$  which contain components of the polar curve. Then the restriction of  $\ell$  to  $X \setminus \bigcup W_{ij}$  is a bilipschitz local homeomorphism by the Very Thin Zone Lemma 3.3. In particular, this set is metrically conical.

Let  $\nu$  be an  $\mathcal{L}$ -node. Then coordinates at the double points of  $E$  on  $E_\nu$  can be chosen so that  $\mathcal{N}(\nu)$  is a connected component of  $\pi^{-1}(X \setminus \bigcup W_{ij})$ . This completes the proof of (1)  $\square$



*Proof of part (2).* Let  $\nu$  be an  $\mathcal{L}$ -node and  $\mu$  an adjacent vertex. We must show that the conical structure we have just proved can be extended to a thick structure over  $N(E_\nu) \cap N(E_\mu)$ . Take local coordinates  $u, v$  at the intersection of  $E_\nu$  and  $E_\mu$  such that  $u = 0$  resp.  $v = 0$  is a local equation for  $E_\nu$  resp.  $E_\mu$ .

By Lemma 5.2 we can choose  $c \in \mathbb{C}$  so that the linear form  $h_2 = z_1 - cz_2$  satisfies  $m_\mu(z_1) < m_\mu(h_2)$ . We change coordinates to replace  $z_2$  by  $h_2$ , which does not change the linear projection  $\ell$ , so we still have that  $m_\nu(z_1) = m_\nu(h_2)$ . So we may assume that in our local coordinates  $z_1 = u^{m_\nu(z_1)}v^{m_\mu(z_1)}$  and  $z_2 = u^{m_\nu(z_1)}v^{m_\mu(h_2)}(a + g(u, v))$  where  $a \in \mathbb{C}^*$  and  $g(0, 0) = 0$ . To higher order, the lines  $v = c$  for  $c \in \mathbb{C}$  project onto radial lines of the form  $z_2 = c'z_1$  and the sets  $|u| = d$  with  $d \in \mathbb{R}^+$  project to horn-shaped real hypersurfaces of the form  $|z_2| = d'|z_1|^{m_\mu(h_2)/m_\mu(z_1)}$ . In particular the image of a small domain of the form

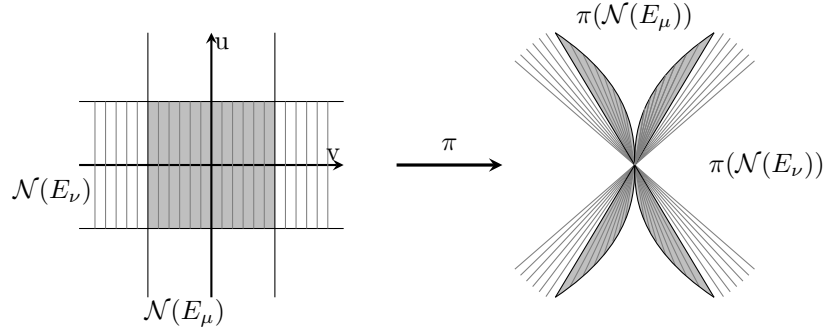


FIGURE 3. Thickness near the boundary of a thick piece

$\{(u, v) : |u| \leq d_1, |v| \leq d_2\}$  is thick. See Figure 3 for a schematic real picture. By the Very Thin Zone Lemma 3.3 the bilipschitz constant remains bounded in this added region, so the desired result again follows by pulling back the standard conical structure from  $\mathbb{C}^2$ .  $\square$

*Proof of part (3).* The proof uses the techniques introduced in Section 12 and will be given there, see Remark 13.4.  $\square$

## 7. FAST LOOPS

We recall the definition of a “fast loop” in the sense of [3], which we will here call sometimes “fast loop of the first kind,” since we also define a closely related concept of “fast loop of the second kind.” We first need another definition.

**Definition 7.1.** If  $M$  is a compact Riemannian manifold and  $\gamma$  a closed rectifiable null-homotopic curve in  $M$ , the *isoperimetric ratio* for  $\gamma$  is the infimum of areas of singular disks in  $M$  which  $\gamma$  bounds, divided by the square of the length of  $\gamma$ .

**Definition 7.2.** Let  $\gamma$  be a closed curve in the link  $X^{(\epsilon_0)} = X \cap S_{\epsilon_0}$ . Suppose there exists a continuous family of loops  $\gamma_\epsilon : S^1 \rightarrow X^{(\epsilon)}$ ,  $\epsilon \leq \epsilon_0$ , whose lengths shrink faster than linearly in  $\epsilon$  and with  $\gamma_{\epsilon_0} = \gamma$ . If  $\gamma$  is homotopically nontrivial in  $X^{(\epsilon_0)}$  we call the family  $\{\gamma_\epsilon\}_{0 < \epsilon \leq \epsilon_0}$  a *fast loop of the first kind* or simply a *fast loop*. If  $\gamma$  is homotopically trivial but the isoperimetric ratio of  $\gamma_\epsilon$  tends to  $\infty$  as  $\epsilon \rightarrow 0$  we call the family  $\{\gamma_\epsilon\}_{0 < \epsilon \leq \epsilon_0}$  a *fast loop of the second kind*.

**Proposition 7.3.** *The existence of a fast loop of the first or second kind is an obstruction to the metric conicalness of  $(X, 0)$ .*

*Proof.* It is shown [3] that a fast loop of the first kind cannot exist in a metric cone, so its existence is an obstruction to metric conicalness.

For a fixed Riemannian manifold  $M$  the isoperimetric ratio for a given nullhomotopic curve is invariant under scaling of the metric and is changed by a factor of at most  $K^4$  by a  $K$ -bilipschitz homeomorphism of  $M$ . It follows that if  $X$  is metrically conical then for any  $C > 0$  there is an overall bound on the isoperimetric ratio of nullhomotopic curves in  $X^{(\epsilon)}$  of length  $\leq C\epsilon$  as  $\epsilon \rightarrow 0$ .  $\square$

**Theorem 7.4.** *Any curve in a Milnor fiber of a thin zone  $Z_j^{(\epsilon_0)}$  of  $X^{(\epsilon_0)}$  which is homotopically nontrivial in  $Z_j^{(\epsilon_0)}$  gives a fast loop of the first or second kind.*

*Proof.* Using the vector field of Proposition 5.1, any closed curve  $\gamma$  in the Milnor fiber of the link  $Z_j^{(\epsilon_0)}$  of a thin piece  $Z_j$  of  $X^{(\epsilon_0)}$  gives rise to a continuous family of closed curves  $\gamma_\epsilon: [0, 1] \rightarrow Z_j^{(\epsilon)}$ ,  $\epsilon \leq \epsilon_0$ , whose lengths shrink faster than linearly with respect to  $\epsilon$ .

If  $\gamma$  is homotopically non-trivial in  $X^{(\epsilon_0)}$  then  $\{\gamma_\epsilon\}_{0 < \epsilon \leq \epsilon_0}$  is a fast loop of the first kind. Otherwise, let  $f: D_\epsilon \rightarrow X^{(\epsilon)}$  be a map of a disc with boundary  $\gamma_\epsilon$ .

Let  $Y = \bigcup_i Y_i$  denotes the thick part of  $X$ . Let  $Y_\epsilon \subset Y$  for  $\epsilon \leq \epsilon_0$  be a collection of conical subsets as in Definition 1.2. The link of  $Y_\epsilon$  is  $Y^{(\epsilon)}$ . We can approximate  $f$  by a smooth map transverse to  $\partial Y^{(\epsilon)}$  while only increasing area by an arbitrarily small factor. Then  $f(D) \cap \partial Y^{(\epsilon)}$  consists of smooth immersed closed curves. A standard innermost disk argument shows that at least one of them is homotopically nontrivial in  $\partial Y^{(\epsilon)}$  and bounds a disk  $D'$  in  $Y^{(\epsilon)}$  obtained by restricting  $f$  to a subdisk of  $D$ . Since there is a lower bound proportional to  $\epsilon$  on the length of essential closed curves in  $\partial Y^{(\epsilon)}$  and  $Y$  is thick, the area of  $D'$  is bounded below proportional to  $\epsilon^2$ . It follows that the isoperimetric ratio for  $\gamma_\epsilon$  tends to  $\infty$  as  $\epsilon \rightarrow 0$ .  $\square$

**Theorem 7.5. 1.** *Every thin piece  $Z_j$  contains a fast loop (of the first kind). In fact every boundary component of a Milnor fiber  $F_j$  of  $Z_j$  is one.*

**2.** *Every point  $p \in Z_j$  lies on some fast loop  $\{\gamma_\epsilon\}_{0 < \epsilon \leq \epsilon_0}$  and every real tangent line to  $Z_j$  is tangent to  $\bigcup_\epsilon \gamma_\epsilon \cup \{0\}$  for some such fast loop.*

*Proof.* Part 2 follows from Part 1 because the link  $Z_j^{(\epsilon_0)}$  is foliated by Milnor fibers and a boundary component of a Milnor fiber  $\phi_j^{-1}(t)$  can be isotoped into a loop  $\gamma$  through any point of the same Milnor fiber. The family  $\{\gamma_\epsilon\}_{0 < \epsilon \leq \epsilon_0}$  obtained from  $\gamma$  using the vector field of Proposition 5.1 is a fast loop whose tangent line is the real line  $L_j \cap \{\arg z_1 = \arg t\}$ .

We will actually prove a stronger result than part 1 of the theorem, since it is needed in Section 14. First we need a remark.

**Remark 7.6.** The monodromy map  $\psi_j: F_j \rightarrow F_j$  for the fibration  $\phi_j$  is a quasi-periodic map, so after an isotopy it has a decomposition into subsurfaces  $F_\nu$  on which  $\phi_j$  has finite order acting with connected quotient, connected by families of annuli which  $\phi_j$  cyclically permutes by a generalized Dehn twist (i.e., some power is a Dehn twist on each annulus of the family). The minimal such decomposition is the Thurston-Nielsen decomposition, which is unique up to isotopy. By [33] each

$F_\nu$  is associated with a node  $\nu$  of  $\Gamma_j$  while each string joining two nodes  $\nu$  and  $\nu'$  of  $\Gamma_j$  corresponds to a  $\phi_j$ -orbit of annuli connecting  $F_\nu$  to  $F_{\nu'}$ . This decomposition of the fiber  $F_j$  corresponds to the minimal decomposition of  $Z_j^{(\epsilon_0)}$  into Seifert fibered pieces  $Z_\nu^{(\epsilon_0)}$ , with thickened tori between them, i.e., the JSJ decomposition.

The following proposition is more general than part 1 of Theorem 7.5 and therefore completes its proof.  $\square$

**Proposition 7.7.** *Each boundary component of a  $F_\nu$  gives a fast loop (of the first kind).*

*Proof.* We assume the contrary, that some boundary component  $\gamma$  of  $F_\nu$  is homotopically trivial in  $X^{(\epsilon_0)}$ . We will derive a contradiction.

Let  $T$  be the component of  $\partial Z_\nu^{(\epsilon_0)}$  which contains  $\gamma$ . Then it is compressible, so it contains an essential curve which bounds a disc to one side of  $T$  or the other. Cutting  $X^{(\epsilon_0)}$  along  $T$  gives a manifold with a compressible boundary torus. But a plumbed manifold-with-boundary given by negative definite plumbing has a compressible boundary component if and only if it is a solid torus, see [31, 28]. So  $T$  separates  $X^{(\epsilon_0)}$  into two pieces, one of which is a solid torus. Call it  $A$ .

**Lemma 7.8.**  *$\gamma$  represents a nontrivial element of  $\pi_1(A)$ .*

*Proof.* Let  $\Gamma_0$  be the subgraph of  $\Gamma$  representing  $A$ , i.e., a component of the subgraph of  $\Gamma$  obtained by removing the edge corresponding to  $T$ . We will attach an arrow to  $\Gamma_0$  where that edge was. Then the marked graph  $\Gamma_0$  is the plumbing graph for the solid torus  $A$ . We note that  $\Gamma_0$  must contain at least one  $\mathcal{L}$ -node, since otherwise  $A$  would have to be  $Z_j^{(\epsilon_0)}$  or a union of pieces of its JSJ decomposition, but this cannot be a solid torus.

We now blow down  $\Gamma_0$  to eliminate all  $(-1)$ -curves. We then obtain a bamboo  $\Gamma'$  with negative definite matrix with an arrow at one extremity. It is the resolution graph of some cyclic quotient singularity  $Q = \mathbb{C}^2/(\mathbb{Z}/p)$  and from this point of view the arrow represents the strict transform of the zero set of the function  $x^p$  on  $Q$ , where  $x, y$  are the coordinates of  $\mathbb{C}^2$ . The Milnor fibers of this function give the meridian discs of the solid torus  $A$ . The intersection of one of them with any curvette (transverse complex disc to an exceptional curve) is positive (namely an entry of the first row of  $pS_{\Gamma'}^{-1}$ , where  $S_{\Gamma'}$  is the intersection matrix associated with  $\Gamma'$ ). Returning back to our initial  $X^{(\epsilon_0)}$ , let  $z_{1*}: H_1(z_1^{-1}(S_{\epsilon_0}^1) \cap X^{(\epsilon_0)}; \mathbb{Z}) \rightarrow \mathbb{Z}$  be the map induced by the Milnor-Lê fibration  $z_1: z_1^{-1}(S_{\epsilon_0}^1) \cap X^{(\epsilon_0)} \rightarrow S_{\epsilon_0}^1$ . Then  $z_{1*}(c) > 0$  for each meridian curve  $c$  of  $A$ . Since  $z_{1*}(\gamma) = 0$ , this implies the lemma.  $\square$

We now know that  $\gamma$  is represented by a non-zero multiple of the core of the solid torus  $A$ . This core curve is the curvette boundary for the curvette transverse to the end curve of the bamboo obtained by blowing down  $\Gamma_0$  in the above proof.

**Lemma 7.9.** *Given any good resolution graph (not necessarily minimal) for a normal complex surface singularity whose link  $\Sigma$  has infinite fundamental group, the boundary of a curvette always represents an element of infinite order in  $\pi_1(\Sigma)$ .*

*Proof.* After blowing down to obtain a minimal good resolution graph the only case to check is when the blown down curvette  $c$  intersects a bamboo, since otherwise its boundary represents a nontrivial element of the fundamental group of some

piece of the JSJ decomposition of  $\Sigma$  and each such piece embeds  $\pi_1$ -injectively in  $\Sigma$ . If  $c$  intersects a single exceptional curve  $E_1$  of the bamboo, then its boundary is homotopic to a positive multiple of the curvette boundary for  $E_1$ , so by the argument in the proof of the previous lemma, the boundary of  $c$  is homotopic to a positive multiple of the core curve of the corresponding solid torus. As a fiber of the Seifert fibered structure on a JSJ component of  $\Sigma$ , this element has infinite order in  $\pi_1$  of the component and therefore of  $\Sigma$ . Finally suppose  $c$  intersects the intersection point of two exceptional divisors  $E_1$  and  $E_2$  of the bamboo. Then in local coordinates  $(u, v)$  with  $E_1 = \{u = 0\}$  and  $E_2 = \{v = 0\}$  the curvette can be given by a Puiseux expansion  $u = \sum_i v^{\frac{q_i}{p_i}}$ , where, without loss of generality,  $q_i > p_i$ . Then the boundary of  $c$  is an iterated torus knot in this coordinate system which homologically is a positive multiple of  $p_1\mu_1 + q_1\mu_2$ , where  $\mu_i$  is a curvette boundary of  $E_i$  for  $i = 1, 2$ . We conclude by applying the previous argument to  $\mu_1$  and  $\mu_2$  that  $c$  is a positive multiple of the core curve of the solid torus, completing the proof.  $\square$

Returning to the proof of Proposition 7.7, we see that if  $\pi_1(X^{(\epsilon_0)})$  is infinite then the curve  $\gamma$  of Lemma 7.8 is nontrivial in  $\pi_1(X^{(\epsilon_0)})$  by Lemma 7.9, proving the proposition in this case.

It remains to prove the proposition when  $\pi_1(X^{(\epsilon_0)})$  is finite. Then  $(X, 0)$  is a rational singularity ([7, 16]), and the link of  $X^{(\epsilon_0)}$  is either a lens space or a Seifert manifold with three exceptional fibers with multiplicities  $(\alpha_1, \alpha_2, \alpha_3)$  equal to  $(2, 3, 3)$ ,  $(2, 3, 4)$ ,  $(2, 3, 5)$  or  $(2, 2, k)$  with  $k \geq 2$ .

We will use the following lemma

**Lemma 7.10.** *Let  $A$  and  $\gamma$  as in Lemma 7.8. Suppose the subgraph  $\Gamma_0$  of  $\Gamma$  representing the solid torus  $A$  is a bamboo*

$$\begin{array}{c} \overset{-b_1}{\circ} \text{---} \overset{-b_2}{\circ} \text{---} \text{---} \text{---} \overset{-b_r}{\circ} \\ \nu_1 \quad \nu_2 \quad \quad \quad \nu_r \end{array}$$

*attached at vertex  $\nu_1$  to the vertex  $\nu$  of  $\Gamma$ . Denote by  $m_\nu$  and  $m_{\nu_1}$  the multiplicities of the function  $\tilde{z}_1 = z_1 \circ \pi$  along  $E_\nu$  and  $E_{\nu_1}$ , and let  $(\alpha, \beta)$  be the Seifert invariant of the core of  $A$  viewed as a singular fiber of the  $S^1$ -fibration over  $E_\nu$ , i.e.,  $\frac{\alpha}{\beta} = [b_{\nu_1}, \dots, b_{\nu_n}]$ . Let  $C$  be the core of  $A$  oriented as the boundary of a curvette of  $E_{\nu_r}$ . Then, with  $d = \gcd(m_\nu, m_{\nu_1})$ , we have*

$$\gamma = \left( \frac{m_{\nu_1}}{d} \alpha - \frac{m_\nu}{d} \beta \right) C \quad \text{in} \quad H_1(A; \mathbb{Z}).$$

*Proof.* Orient the torus  $T$  as a boundary component of  $A$ . Let  $C_\nu$  and  $C_{\nu_1}$  in  $T$  be boundaries of curvettes of  $E_\nu$  and  $E_{\nu_1}$ . Then  $\gamma = \frac{m_\nu}{d} C_{\nu_1} - \frac{m_{\nu_1}}{d} C_\nu$ , and the meridian of  $A$  on  $T$  is given by  $M = \alpha C_{\nu_1} + \beta C_\nu$ . Then  $\gamma = \lambda C$  where  $\lambda = M \cdot \gamma$ . As  $C_{\nu_1} \cdot C_\nu = +1$  on  $T$ , we then obtain the stated formula.  $\square$

Let us return to the proof of Proposition 7.7. When  $X^{(\epsilon_0)}$  is a lens space, then the minimal resolution graph is a bamboo:

$$\begin{array}{c} \overset{-b_1}{\circ} \text{---} \overset{-b_2}{\circ} \text{---} \text{---} \text{---} \overset{-b_n}{\circ} \end{array}$$

The function  $\tilde{z}_1$  has multiplicity 1 along each  $E_i$ , and the strict transform of  $z_1$  has  $b_1 - 1$  components intersecting  $E_1$ ,  $b_n - 1$  components on  $E_n$ , and  $b_i - 2$  components on any other curve  $E_i$ . In particular the  $\mathcal{L}$ -nodes are the two extremal vertices of the bamboo and any vertex with  $b_i \geq 3$ . To get the adapted resolution graph of

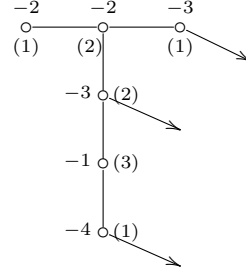
section 2 we should blow up once between any two adjacent  $\mathcal{L}$ -nodes. Then the subgraph  $\Gamma_j$  associated with our thin piece  $Z_j$  is either a  $(-1)$ -weighted vertex or a maximal string  $\nu_i, \nu_{i+1}, \dots, \nu_k$  of vertices excluding  $\nu_1, \nu_n$  carrying self intersections  $b_j = -2$ .

We first consider the second case. Let  $\gamma$  be the intersection of the Milnor fiber of  $Z_j$  with the plumbing torus at the intersection of  $E_k$  and  $E_{k+1}$ . According to Lemma 7.10, we have  $\gamma = (\alpha - \beta)C$  where  $C$  is the boundary of a curvette of  $E_n$  and  $\frac{\alpha}{\beta} = [b_{k+1}, \dots, b_n]$  with  $E_i^2 = -b_i$ . But  $C$  is a generator of the cyclic group  $\pi_1(X^{(\epsilon_0)})$ , which has order  $p = [b_1, \dots, b_n]$ . Since  $0 < \alpha - \beta \leq \alpha < p$ , we obtain that  $\gamma$  is nontrivial in  $\pi_1(X^{(\epsilon_0)})$ .

For the case of a  $(-1)$ -vertex we can work in the minimal resolution with  $E_k$  and  $E_{k+1}$  the two adjacent  $\mathcal{L}$ -curves and  $T$  the plumbing torus at their intersection, since blowing down the  $(-1)$ -curve does not change  $\gamma$ . So it is the same calculation as before. This completes the lens space case.

We now assume that  $X^{(\epsilon_0)}$  has three exceptional fibers whose multiplicities  $(\alpha_1, \alpha_2, \alpha_3)$  are  $(2, 3, 3)$ ,  $(2, 3, 4)$ ,  $(2, 3, 5)$  or  $(2, 2, k)$  with  $k \geq 2$ . Then the graph  $\Gamma$  is star-shaped with three branches and with a central node whose Euler number is  $e \leq -2$ . If  $e \leq -3$ , then  $\tilde{z}_1$  has multiplicity 1 on each exceptional curve and we conclude using Lemma 7.10 as in the lens space case.

When  $e = -2$ , then the multiplicities of  $\tilde{z}_1$  are not all equal to 1, and we have to examine all the cases one by one. For  $(\alpha_1, \alpha_2, \alpha_3) = (2, 3, 5)$ , there are eight possible values for the Seifert pairs, which are  $(2, 1)$ ,  $(3, \beta_2)$ ,  $(5, \beta_3)$  where  $\beta_2 \in \{1, 2\}$  and  $\beta_3 \in \{1, 2, 3, 4\}$ . For example, in the case  $\beta_2 = 1$  and  $\beta_3 = 3$  the resolution graph  $\Gamma$  is represented by



The arrows represent the strict transform of the generic linear function  $z_1$ . There are two thin zones obtained by deleting the vertices with arrows and their adjacent edges, leading to four curves  $\gamma$  to be checked. Lemma 7.10 computes them as  $C_3$ ,  $2C_5$ ,  $C_5$  and  $C_5$  respectively, where  $C_p$  is the exceptional fiber of degree  $p$ . The other cases are easily checked in the same way. The case  $(2, 2, k)$  gives an infinite family similar to the lens space case.  $\square$

Proposition 7.3 and either one of Theorem 7.4 or Theorem 7.5 show:

**Corollary 7.11.**  *$(X, 0)$  is metrically conical if and only if there are no thin pieces. Equivalently,  $\Gamma$  has only one node, and it is the unique  $\mathcal{L}$ -node.*  $\square$

**Example 7.12.** Let  $(X, 0) \subset (\mathbb{C}^3, 0)$ , defined by  $x^a + y^b + z^b = 0$  with  $1 \leq a < b$ . Then the graph  $\Gamma$  is star-shaped with  $b$  bamboos and the single  $\mathcal{L}$ -node is the central vertex. Therefore,  $(X, 0)$  is metrically conical. This metric conicalness was first proved in [4].

## 8. UNIQUENESS OF THE MINIMAL THICK-THIN DECOMPOSITION

We first prove:

**Lemma 8.1.** *The thick-thin decomposition constructed in Section 2 is minimal, as defined in Definition 1.5.*

*Proof.* Any real tangent line to  $Z_j$  is a tangent line to some fast loop  $\{\gamma_\epsilon\}_{0 < \epsilon \leq \epsilon_0}$  by Theorem 7.5. For any other thick-thin decomposition this fast loop is outside any conical part of the thick part for all sufficiently small  $\epsilon$  so its tangent line is a tangent line to a thin part. It follows that this thick-thin decomposition contains a thin piece which is tangent to the tangent cone of  $Z_j$ . Thus the first condition of minimality is satisfied. For the second part, note that any thick-thin decomposition must have a thin piece close to each  $Z_j$  because of the above fast loops, so it has at least as many thin pieces as the constructed one.  $\square$

We restate the Uniqueness Theorem of the Introduction:

**Theorem (1.7).** *A minimal thick-thin decomposition is canonical, in the sense that it is isotopic to any other minimal thick-thin decomposition.*

*Proof.* It follows from the proof of Lemma 8.1 that any two minimal thick-thin decompositions have the same numbers of thick and thin pieces. Let us consider the thick-thin decomposition

$$(X, 0) = \bigcup_{i=1}^r (Y_i, 0) \cup \bigcup_{j=1}^s (Z_j, 0)$$

constructed in Section 2 and another minimal thick-thin decomposition

$$(X, 0) = \bigcup_{i=1}^r (Y'_i, 0) \cup \bigcup_{j=1}^s (Z'_j, 0).$$

They can be indexed so that for each  $j$  the intersection  $Z_j \cap Z'_j \cap (B_\epsilon \setminus \{0\})$  is non-empty for all small  $\epsilon$  (this is not hard to see, but in fact we only need that  $Z_j$  and  $Z'_j$  are very close to each other in the sense that the distance between  $Z_j \cap S_\epsilon$  and  $Z'_j \cap S_\epsilon$  is bounded by  $c\epsilon^q$  for some  $c > 0$  and  $q > 1$ , which is immediate from the proof of Lemma 8.1).

Definition 1.2 says  $Y = \bigcup_i Y_i$  is the union of metrically conical subsets  $Y_\epsilon \subset B_\epsilon$ ,  $0 < \epsilon \leq \epsilon_0$ . We will denote by  $\partial_0 Y_\epsilon := \overline{\partial Y_\epsilon} \setminus (Y_\epsilon \cap S_\epsilon)$ , the “sides” of these cones, which form a disjoint union of cones on tori. We do the same for  $Y' = \bigcup_i Y'_i$ .

The limit as  $\epsilon \rightarrow 0$  of the tangent cones of any component of  $\partial_0 Y_\epsilon$  is the tangent line to a  $Z_j$ . It follows that for all  $\epsilon_1$  sufficiently small  $\partial_0 Y'_{\epsilon_1}$  will be “outside”  $\partial_0 Y_{\epsilon_0}$  in the sense that is disjoint from  $Y_{\epsilon_0}$  except at 0. So choose  $\epsilon_1 \leq \epsilon_0$  so this is so. Similarly, choose  $0 < \epsilon_3 \leq \epsilon_2 \leq \epsilon_1$  so that  $\partial_0 Y_{\epsilon_2}$  is outside  $\partial_0 Y'_{\epsilon_1}$  and  $\partial_0 Y'_{\epsilon_3}$  is outside  $\partial_0 Y_{\epsilon_2}$ .

Now consider the 3-manifold  $M \subset S_{\epsilon_3}$  consisting of what is between  $\partial_0 Y_{\epsilon_0}$  and  $\partial_0 Y'_{\epsilon_3}$  in  $X \cap S_{\epsilon_3}$ . We can write  $M$  as  $M_1 \cup M_2 \cup M_3$  where  $M_1$  is between  $\partial_0 Y_{\epsilon_0}$  and  $\partial_0 Y'_{\epsilon_1}$ ,  $M_2$  between  $\partial_0 Y'_{\epsilon_1}$  and  $\partial_0 Y_{\epsilon_2}$  and  $M_3$  between  $\partial_0 Y_{\epsilon_2}$  and  $\partial_0 Y'_{\epsilon_3}$ . Each component of  $M_1 \cup M_2$  is homeomorphic to  $\partial_1 M_2 \times I$  and each component of  $M_2 \cup M_3$  is homeomorphic to  $\partial_0 M_2 \times I$ , so it follows by a standard argument that each component of  $M_2$  is homeomorphic to  $\partial_0 M_2 \times I$  ( $M_2$  is an invertible bordism

between its boundaries and apply Stallings's h-cobordism theorem [36]; alternatively, use Waldhausen's classification of incompressible surfaces in  $surface \times I$  in [38]).

The complement of the  $\epsilon_3$ -link of  $Y_{\epsilon_2}$  in  $X^{(\epsilon_3)}$  is the union of  $Z^{(\epsilon_3)}$  and a collar neighborhood of its boundary and is hence isotopic to  $Z^{(\epsilon_3)}$ . It is also isotopic to its union with  $M_2$  which is the complement of the  $\epsilon_3$ -link of  $Y'_{\epsilon_1}$ . This latter is  $(Z')^{(\epsilon_3)}$  union a collar, and is hence isotopic to  $(Z')^{(\epsilon_3)}$ . Thus the links of  $Z$  and  $Z'$  are isotopic, so  $Z$  and  $Z'$  are isotopic.  $\square$

We can also characterize, as in the following theorem, the unique minimal thick-thin decomposition in terms of the analogy with the Margulis thick-thin decomposition mentioned in the Introduction. The proof is immediate from the proof of Lemma 8.1.

**Theorem 8.2.** *The canonical thick-thin decomposition can be characterized among thick-thin decompositions by the following condition: For any sufficiently small  $q > 1$  there exists  $\epsilon_0 > 0$  such that for all  $\epsilon \leq \epsilon_0$  any point  $p$  of the thin part with  $|p| < \epsilon$  is on an essential loop in  $X \setminus \{0\}$  of length  $\leq |p|^q$ .*  $\square$

In fact one can prove more (but we will not do so here): the set of points which are on essential loops as in the above theorem gives the thin part of a minimal thick-thin decomposition when intersected with a sufficiently small  $B_\epsilon$ .

We have already pointed out that the thick-thin decomposition is an invariant of semi-algebraic bilipschitz homeomorphism. But in fact, if one makes an arbitrary  $K$ -bilipschitz change to the metric on  $X$ , the thin pieces can still be recovered up to homeomorphism using the construction of the previous paragraph plus some 3-manifold topology to tidy up the result. Again, we omit details.

## 9. METRIC TANGENT CONE

The thick-thin decomposition gives a description of the metric tangent cone of Bernig and Lytchak [1] for a normal complex surface germ. The *metric tangent cone*  $\mathcal{T}_0 A$  is defined for any real semialgebraic germ  $(A, 0) \subset (\mathbb{R}^N, 0)$  as the Gromov-Hausdorff limit

$$\mathcal{T}_0 A := \lim_{\epsilon \rightarrow 0}^{\text{gh}} \left( \frac{1}{\epsilon} A, 0 \right),$$

where  $\frac{1}{\epsilon} A$  means  $A$  with its inner metric scaled by a factor of  $\frac{1}{\epsilon}$ .

As a metric germ  $\mathcal{T}_0 A$  is the strict cone on its link  $\mathcal{T}_0 A^{(1)} := \mathcal{T}_0 A \cap S_1$ , and

$$\mathcal{T}_0 A^{(1)} = \lim_{\epsilon \rightarrow 0}^{\text{gh}} \frac{1}{\epsilon} A^{(\epsilon)},$$

where  $\frac{1}{\epsilon} A^{(\epsilon)}$  is the link of radius  $\epsilon$  of  $(A, 0)$  scaled to lie in the unit sphere  $S_1 \subset \mathbb{R}^N$ .

Applying this to  $(X, 0) \subset \mathbb{C}^n$ , we see that the thin zones collapse to circles as  $\epsilon \rightarrow 0$ . In particular, the boundary tori of each Seifert manifold link  $\frac{1}{\epsilon} Y_i^{(\epsilon)}$  of a thick zone collapse to the same circles, so that in the limit we have a “branched Seifert manifold” (where branching of  $k > 1$  sheets of the manifold meeting along a circle occurs if the collapsing map of a boundary torus to  $S^1$  has fibers consisting of  $k > 1$  circles). Therefore, the link  $\mathcal{T}_0 X^{(1)}$  of the metric tangent cone is the union of the branched Seifert manifolds glued along the circles to which the thin zones have collapsed.

The ordinary tangent cone  $T_0 X$  and its link  $T_0 X^{(1)}$  can be similarly constructed as the Hausdorff limit of  $\frac{1}{\epsilon} X$  resp.  $\frac{1}{\epsilon} X^{(\epsilon)}$  (as embedded metric spaces in  $\mathbb{C}^n$  resp.

the unit sphere  $S_1$ ). In particular, there is a canonical finite-to-one projection  $\mathcal{T}_0X \rightarrow T_0X$  (described in the more general semi-algebraic setting in [1]), whose degree over a general point  $p \in T_0X$  is the multiplicity of  $T_0X$  at that point. This is a branched cover, branched over the exceptional tangent lines in  $T_0X$ .

The circles to which thin zones collapse map to the links of some of these exceptional tangent lines, but there can also be branching in the part of  $\mathcal{T}_0X$  corresponding to the thick part of  $X$ ; such branching corresponds to bamboos on  $\mathcal{L}$ -nodes of the resolution of  $X$ . Summarizing:

**Theorem 9.1.** *The metric tangent cone  $\mathcal{T}_0X$  is a branched cover of the tangent cone  $T_0X$ , branched over the exceptional lines in  $T_0X$ . It has a natural complex structure (lifted from  $T_0X$ ) as a non-normal complex surface. Removing a finite set of complex lines (corresponding to thin zones) results in a complex surface which is homeomorphic to the interior of the thick part of  $X$  by a homeomorphism which is bilipschitz outside an arbitrarily small cone neighborhood of the removed lines.  $\square$*

## Part II: The bilipschitz classification

The remainder of the paper builds on the thick thin decomposition to complete the bilipschitz classification, as described in Theorem 1.9.

### 10. THE REFINED DECOMPOSITION OF $(X, 0)$

The decomposition of  $(X, 0)$  for the Classification Theorem 1.9 was described there in terms of the link  $X^{(\epsilon)}$  as follows: first refine the thick-thin decomposition  $X^{(\epsilon)} = \bigcup_{i=1}^r Y_i^{(\epsilon)} \cup \bigcup_{j=1}^s Z_j^{(\epsilon)}$  by decomposing each thin zone  $Z_j^{(\epsilon)}$  into its JSJ decomposition (minimal decomposition into Seifert fibered manifolds glued along their boundaries) while leaving the thick zones  $Y_i^{(\epsilon)}$  as they are; then thicken some of the gluing tori of this refined decomposition to collars  $T^2 \times I$ . We will call the latter *special annular pieces*.

In this section we describe where these special annular pieces are added, to complete the description of the data (1) of Theorem 1.9.

We consider a generic linear projection  $\ell: (X, 0) \rightarrow (\mathbb{C}^2, 0)$  and we denote again by  $\Pi$  its polar curve and by  $\Pi^*$  the strict transform with respect to the resolution defined in Section 2. Before adding the special annular pieces, each piece of the above refined decomposition is either a thick zone, corresponding to an  $\mathcal{L}$ -node of our resolution graph  $\Gamma$ , or a Seifert fibered piece of the minimal decomposition of a thin zone, which corresponds to a  $\mathcal{T}$ -node of  $\Gamma$ . The incidence graph for this decomposition is the graph whose vertices are the nodes of  $\Gamma$  and whose edges are the maximal strings  $\sigma$  between nodes. We add a special annular piece corresponding to a string  $\sigma$  if and only if  $\Pi^*$  meets an exceptional curve belonging to this string.

This refines the incidence graph of the decomposition by adding a vertex on each edge which gives a special annular piece. As in the Introduction, we call this graph  $\Gamma_0$ . We then have a decomposition

$$(14) \quad X^{(\epsilon)} = \bigcup_{\nu \in V(\Gamma_0)} M_\nu^{(\epsilon)},$$

into Seifert fibered pieces, some of which are special annular.

In the next section we will use this decomposition, together with the additional data described in Theorem 1.9, to construct a bilipschitz model for  $(X, 0)$ . To do



so we will need to modify decomposition (14) by replacing each separating torus of the decomposition by a toral annulus  $T^2 \times I$ :

$$(15) \quad X^{(\epsilon_0)} = \bigcup_{\nu \in V(\Gamma_0)} M_\nu^{(\epsilon_0)} \cup \bigcup_{\sigma \in E(\Gamma_0)} A_\sigma^{(\epsilon_0)}.$$

At this point the only data of Theorem 1.9 which have not been described are the weights  $q_\nu$  of part (3). These are certain Puiseux exponents of the discriminant curve  $\Delta$  of the generic plane projection of  $X$ , and will be revealed in sections 12 and 13, where we show that  $X$  is bilipschitz homeomorphic to its bilipschitz model. Finally, we prove that the data are bilipschitz invariants of  $(X, 0)$  in Section 14.

## 11. THE BILIPSCHITZ MODEL OF $(X, 0)$

We describe how to build a bilipschitz model for a normal surface germ  $(X, 0)$  by gluing individual pieces using the data of Theorem 1.9. Each piece will be topologically the cone on some manifold  $N$  and we call the subset which is the cone on  $\partial N$  the *cone-boundary* of the piece. The pieces will be glued to each other along their cone-boundaries using isometries. We first define the pieces.

**Definition 11.1** ( $A(q, q')$ ). Here  $1 \leq q < q'$  are rational numbers.

Let  $A$  be the euclidean annulus  $\{(\rho, \psi) : 1 \leq \rho \leq 2, 0 \leq \psi \leq 2\pi\}$  in polar coordinates and for  $0 < r \leq 1$  let  $g_{q, q'}^{(r)}$  be the metric on  $A$ :

$$g_{q, q'}^{(r)} := (r^q - r^{q'})^2 d\rho^2 + ((\rho - 1)r^q + (2 - \rho)r^{q'})^2 d\psi^2.$$

So  $A$  with this metric is isometric to the euclidean annulus with inner and outer radii  $r^{q'}$  and  $r^q$ . The metric completion of  $(0, 1] \times S^1 \times A$  with the metric

$$dr^2 + r^2 d\theta^2 + g_{q, q'}^{(r)}$$

compactifies it by adding a single point at  $r = 0$ . We call the result  $A(q, q')$ .

(To make the comparison with the local metric of Nagase [30] clearer we note that this metric is bilipschitz equivalent to  $dr^2 + r^2 d\theta^2 + r^{2q}(ds^2 + (r^{q' - q} + s)^2)d\psi^2$  with  $s = \rho - 1$ .)

**Definition 11.2** ( $B(F, \phi, q)$ ). Let  $F$  be a compact oriented 2-manifold,  $\phi: F \rightarrow F$  an orientation preserving diffeomorphism, and  $F_\phi$  the mapping torus of  $\phi$ , defined as:

$$F_\phi := ([0, 2\pi] \times F) / ((2\pi, x) \sim (0, \phi(x))).$$

Given a rational number  $q > 1$  we will define a metric space  $B(F, \phi, q)$ , which is topologically the cone on the mapping torus  $F_\phi$ .

For each  $0 \leq \theta \leq 2\pi$  choose a Riemannian metric  $g_\theta$  on  $F$ , varying smoothly with  $\theta$ , such that for some small  $\delta > 0$ :

$$g_\theta = \begin{cases} g_0 & \text{for } \theta \in [0, \delta], \\ \phi^* g_0 & \text{for } \theta \in [2\pi - \delta, 2\pi]. \end{cases}$$

Then for any  $r \in (0, 1]$  the metric  $r^2 d\theta^2 + r^{2q} g_\theta$  on  $[0, 2\pi] \times F$  induces a smooth metric on  $F_\phi$ . Thus

$$dr^2 + r^2 d\theta^2 + r^{2q} g_\theta$$

defines a smooth metric on  $(0, 1] \times F_\phi$ . The metric completion of  $(0, 1] \times F_\phi$  adds a single point at  $r = 0$ . Denote this completion by  $B(F, \phi, q)$ ; it can be thought of as a “globalization” of the local metric of Hsiang and Pati [15].

Note that changing  $\phi$  by an isotopy or changing the initial choice of the family of metrics on  $F$  does not change the bilipschitz class of  $B(F, \phi, q)$ . It will be convenient to make some additional choices. For a boundary component  $\partial_i F$  of  $F$  let  $m_i(F)$  be the smallest  $m > 0$  for which  $\phi^m(\partial_i F) = \partial_i F$ . By changing  $\phi$  by an isotopy if necessary and choosing the  $g_\theta$  suitably we may assume:

- $\phi^{m_i(F)}$  is the identity on  $\partial_i F$  for each  $i$ ;
- in a neighbourhood of  $\partial F$  we have  $g_\theta = g_0$  for all  $\theta$ ;
- the lengths of the boundary components of  $F$  are  $2\pi$ .

Then the metric  $r^2 d\theta^2 + r^{2q} g_\theta$  on the boundary component of  $F_\phi$  corresponding to  $\partial_i F$  is the product of a circle of circumference  $2\pi m' r$  and one of circumference  $2\pi r^q$ .

**Definition 11.3** (*CM*). Given a compact smooth 3-manifold  $M$ , choose a Riemannian metric  $g$  on  $M$  and consider the metric  $dr^2 + r^2 g$  on  $(0, 1] \times M$ . The completion of this adds a point at  $r = 0$ , giving a *metric cone on  $M$* . The bilipschitz class of this metric is independent of choice of  $g$ , and we will choose it later to give the boundary components of  $M$  specific desired shapes.

A piece bilipschitz equivalent to  $A(q, q')$  will also be said to be of type  $A(q, q')$  and similarly for types  $B(F, \phi, q)$  and *CM*. We now describe how to glue together pieces of these three types to obtain our bilipschitz model for  $(X, 0)$ . Note that, although we are only interested in metrics up to bilipschitz equivalence, we must glue pieces by strict isometries of their cone-boundaries. In order that the cone-boundaries are strictly isometric, we may need to change the metric in Definition 11.2 or 11.3 by replacing the term  $r^2 d\theta^2$  by  $m^2 r^2 d\theta^2$  for some positive integer  $m$ . This gives the same metric up to bilipschitz equivalence.

For example, given  $F$ ,  $\phi$ ,  $q$  and  $q'$ , each component  $C$  of the cone-boundary of  $B(F, \phi, q)$  is isometric to the left boundary component of  $A(q, q')$  after altering the metrics on  $B(F, \phi, q)$  and  $A(q, q')$  as just described, using  $m$  equal to the number of components of  $F$  and the number of components of  $F \cap C$  respectively. So we can glue  $B(F, \phi, q)$  to  $A(q, q')$  along  $C$ , giving a manifold with piecewise smooth metric. Similarly, a piece  $B(F, \phi, q')$  can be glued to the right boundary of  $A(q, q')$ . Finally, since the left boundary of a piece  $A(1, q')$  is strictly conical, it can be glued to a boundary component of a conical piece *CM* (again, after suitably adjusting the metric to be correct on the appropriate boundary component of  $M$ ).

Consider now the decomposition (15) of the previous section, which is the decomposition of part (1) of Theorem 1.9 but with the gluing tori thickened to annular pieces. We consider also the weights  $q_\nu$  of part (3) of Theorem 1.9.

Recall that, except for adding annular pieces, this decomposition is obtained from the thick-thin decomposition by JSJ-decomposing the thin zones. Any JSJ decomposition can be positioned uniquely up to isotopy to be transverse to the foliation by fibers of a foliation over  $S^1$  (so long as the leaves are not tori). In particular, this applies to the foliation of part (2) of Theorem 1.9, so we have a foliation with compact leaves on each non-thick piece of this decomposition. For a piece  $A_\sigma^{(\epsilon_0)}$  the leaves are annuli and we define

$$\widehat{A}_\sigma := A(q_\nu, q_{\nu'}),$$

where  $\nu$  and  $\nu'$  are nodes at the ends of the string  $\sigma$ , ordered so that  $q_\nu < q_{\nu'}$ . For a non-thick piece  $M_\nu^{(\epsilon)}$  the leaves are fibers of a fibration  $M_\nu^{(\epsilon)} \rightarrow S^1$ . In this case

let  $\phi_\nu: F_\nu \rightarrow F_\nu$  be the monodromy map of this fibration and define

$$\widehat{M}_\nu := B(F_\nu, \phi_\nu, q_\nu).$$

Finally, for each node  $\nu$  of  $\Gamma$  such that  $q_\nu = 1$  (i.e.,  $M_\nu^{(\epsilon)}$  is thick) we define

$$\widehat{M}_\nu := CM_\nu^{(\epsilon)}.$$

We can glue together the pieces  $\widehat{M}_\nu$  and  $\widehat{A}_\sigma$  according to the topology of the decomposition  $X^{(\epsilon)} = \bigcup_\nu M_\nu^{(\epsilon)} \cup \bigcup_\sigma A_\sigma^{(\epsilon)}$ , arranging, as described above, that the gluing is by isometries of the cone-boundaries. We can also make sure that the foliations match to give the foliations of the thin zones (item (2) of Theorem 1.9). We obtain a semialgebraic set

$$(\widehat{X}, 0) = \bigcup_\nu (\widehat{M}_\nu, 0) \cup \bigcup_\sigma (\widehat{A}_\sigma, 0).$$

The next two sections prove that  $(\widehat{X}, 0) \cong (X, 0)$  (bilipschitz equivalence) while determining the  $q_\nu$ 's of item (3) of Theorem 1.9 in the process. The proof of the theorem will then be completed in the following Section 14 by showing that the data of Theorem 1.9 are bilipschitz invariants of  $(X, 0)$ .

## 12. THE CARROUSEL DECOMPOSITION OF A THIN PIECE

Let  $\Gamma_j$  be a Tjurina component of  $\Gamma$  and set  $W_j = \pi(N(\Gamma_j))$ . Notice that  $W_j$  is  $Z_j$  plus a collar.

We assume as usual that  $\ell = (z_1, z_2)$  is a generic linear projection. We consider the restriction  $\ell = (z_1, z_2): W_j \rightarrow \mathbb{C}^2$  and we denote by  $\Pi_j \subset W_j$  the polar curve for this projection and  $\Delta_j = \ell(\Pi_j) \subset \mathbb{C}^2$  the discriminant curve. There is a unique  $\lambda_j$  such that  $f_j := z_2 - \lambda_j z_1$  vanishes to greater order on the exceptional curves associated with  $\Gamma_j$  than  $z_1$  (see 5.2). If  $(x, y)$  are the coordinates in  $\mathbb{C}^2$ ,  $\Delta_j$  is tangent to the line  $y = \lambda_j x$ . We change our coordinates for  $\ell$ , replacing  $z_2$  by  $f_j$ , in order that this tangent line is the  $x$  axis.

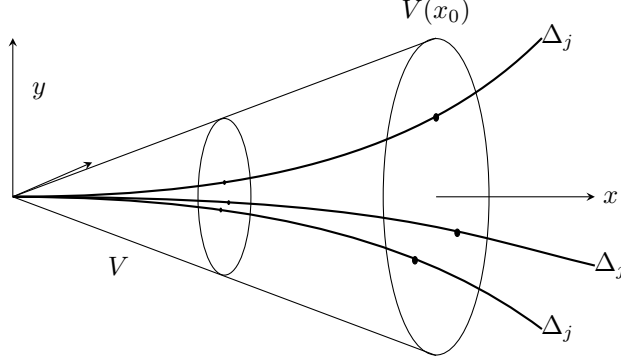
We will work inside the Milnor ball with corners,  $B_\epsilon$ , defined in Section 4. We can assume that the image of  $W_j$  is a cone  $V = \{(x, y) : |x| \leq \epsilon, |y| \leq \eta|x|\} \subset \mathbb{C}^2$  and  $W_j$  is a branched cover of this cone, branched over  $\Delta_j$ . Note that the genericity assumption implies that the branching over  $\Delta_j$  is generic, i.e., the inverse image of a connected neighborhood  $N$  of a point of  $\Delta_j$  has one component which is a double branched cover of  $N$  and all other components map homeomorphically to  $N$ .

Following the ideas of Lê [19] (see also [22]), we now construct a “carrousel decomposition” of  $V$  with respect to the branches of  $\Delta_j$ . It will consist of closures of regions between successively smaller neighborhoods of the successive Puiseux approximations of the branches of  $\Delta_j$ . As such, it is finer than the one of [19], which only needed the first Puiseux pairs of the branches of  $\Delta_j$ .

For simplicity we assume first that  $\Delta_j$  has just one branch. The curve  $\Delta_j$  admits a Puiseux series expansion of the form

$$y = \sum_{i \geq 1} a_i x^{p_i} \in \mathbb{C}\{x^{\frac{1}{N}}\}.$$

Recall that a Puiseux exponent  $p_\xi$  is *characteristic* if the embedded topology of the plane curves  $y = \sum_{i=1}^{\xi-1} a_i x^{p_i}$  and  $y = \sum_{i=1}^{\xi} a_i x^{p_i}$  differ; equivalently  $\text{denom}(p_\xi)$  does not divide  $\text{lcm}_{i < \xi} \{\text{denom}(p_i)\}$ . Let  $p_r$  be the last characteristic exponent.

FIGURE 4. The cone  $V$  and the curve  $\Delta_j$ 

For each  $k \leq r$  choose  $\alpha_k, \beta_k, \gamma_k > 0$  with  $\alpha_k < |a_k| - \gamma_k < |a_k| + \gamma_k < \beta_k$  and consider the region

$$B_k := \left\{ (x, y) : \alpha_k |x^{p_k}| \leq |y - \sum_{i=1}^{k-1} a_i x^{p_i}| \leq \beta_k |x^{p_k}|, |y - \sum_{i=1}^k a_i x^{p_i}| \geq \gamma_k |x^{p_k}| \right\}.$$

If the  $\epsilon$  of our Milnor ball is small enough the  $B_j$ 's will be pairwise disjoint. Denote by  $A_1$  the closure of the region between  $\partial V$  and  $B_1$  and  $A_i$  the closure of the region between  $B_{i-1}$  and  $B_i$  for  $i = 1, \dots, r$ . Finally let  $D$  be

$$D := V \setminus \left( \bigcup_{i=1}^r A_i \cup \bigcup_{i=1}^r B_i \right),$$

Which is the union of connected pieces  $D_1, \dots, D_r, D_{r+1}$ , disjoint except at 0, and indexed so that  $D_k$  is adjacent to  $B_k$  and  $D_{r+1}$  intersects  $\Delta$ .

Then, for  $k = 1, \dots, r$ ,  $A_k$  is bilipschitz equivalent to  $A(p_{k-1}, p_k)$  (Definition 11.1; we put  $p_0 = 1$ ), and  $B_k$  is bilipschitz equivalent to  $B(F_k, \phi_k, p_k)$  (Definition 11.2), where  $F_k$  is a planar surface with  $2 + (\text{lcm}_{i \leq k} \{\text{denom}(p_i)\}) / (\text{lcm}_{i < k} \{\text{denom}(p_i)\})$  boundary components and  $\phi_k$  is a finite order diffeomorphism. Finally, each  $D_k$  is bilipschitz to  $B(D^2, id, p_k)$ .

More generally, if  $\Delta_j$  has several components, we first truncate the Puiseux series for each component of  $\Delta_j$  at a point where truncation does not affect the topology of  $\Delta_j$  (i.e., we truncate at the last term which is either characteristic or coincidence in the sense of e.g., [21]). Then for each pair  $\kappa = (f, p_k)$  consisting of a Puiseux polynomial  $f = \sum_{i=1}^{k-1} a_i x^{p_i}$  and an exponent  $p_k$  for which  $f = \sum_{i=1}^k a_i x^{p_i}$  is a partial sum of the truncated Puiseux series of some component of  $\Delta_j$ , we consider all components of  $\Delta_j$  which fit this data. If  $a_{k1}, \dots, a_{kt}$  are the coefficients of  $x^{p_k}$  which occur in these Puiseux polynomials we define

$$B_\kappa := \left\{ (x, y) : \alpha_\kappa |x^{p_k}| \leq |y - \sum_{i=1}^{k-1} a_i x^{p_i}| \leq \beta_\kappa |x^{p_k}| \right. \\ \left. |y - (\sum_{i=1}^{k-1} a_i x^{p_i} + a_{kj} x^{p_k})| \geq \gamma_\kappa |x^{p_k}| \text{ for } j = 1, \dots, t \right\}.$$

Here  $\alpha_\kappa, \beta_\kappa, \gamma_\kappa$  are chosen so that  $\alpha_\kappa < |a_{kj}| - \gamma_\kappa < |a_{kj}| + \gamma_\kappa < \beta_\kappa$  for each  $j = 1, \dots, t$ . Again, if the  $\epsilon$  of our Milnor ball is small enough the sets  $B_\kappa$  will be disjoint for different  $\kappa$ , and each is again bilipschitz equivalent to some  $B(F, \phi, p_k)$  with  $\phi$  of finite order. The closure of the complement in  $V$  of the union of the  $B_\kappa$ 's is again a union of pieces bilipschitz equivalent to some  $A(q, q')$  or some  $B(D^2, id, q)$ .

The carrousel picture is the picture of the intersection of this decomposition with the plane  $x = \epsilon$ . Figure 5 shows this picture for a discriminant  $\Delta_j$  having two branches with Puiseux expansions respectively  $y = ax^{4/3} + bx^{13/6} + \dots$  and  $y = cx^{7/4} + \dots$ . Note that the intersection of a piece of the decomposition of  $V$  with the disk  $V \cap \{x = \epsilon\}$  will usually have several components.

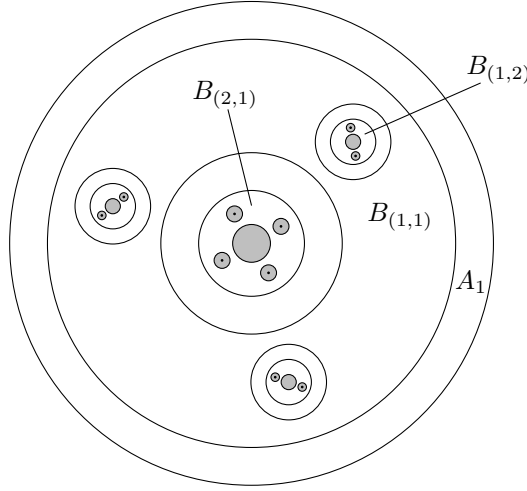
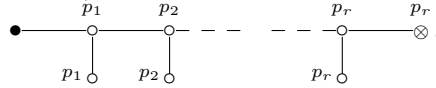


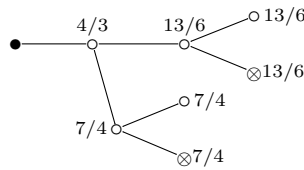
FIGURE 5. Carrousel section for  $\Delta = \{y = ax^{4/3} + bx^{13/6} + \dots\} \cup \{y = cx^{7/4} + \dots\}$ . The region  $D$  is gray.

Consider the incidence graph  $T_j$  for the decomposition of  $V$ , with the vertices for  $B$ - and  $D$ -pieces weighted by their corresponding  $q$ 's. It is a tree, with a root representing  $A_1$ . We delete vertices corresponding to the  $A(q, q')$  pieces other than  $A_1$ , since the presence of such pieces can be seen from edges between vertices with different  $q$ -weights.

For example, in the situation where  $\Delta_j$  is connected, this graph  $T_j$  is a string with leaves corresponding to the  $D_k$ 's attached at the non-root vertices (we mark the root vertex as a filled dot and the piece  $D_{r+1}$  which contain a component of the discriminant with a cross):



For the example of Figure 5 the tree is:



We now lift the decomposition to  $W_j$  by  $\ell$ .

**Lemma 12.1. 1.** *The inverse image of an  $A(q, q')$  piece is a disjoint union of one or more  $A(q, q')$  pieces.*

**2.** *The inverse image of a  $B(F, \phi, q)$  piece is a disjoint union of pieces of type  $B(F, \phi, q)$  (with the same  $q$  but usually different  $F$ 's and  $\phi$ 's), and the  $\phi$ 's for these pieces have finite order, so their links are Seifert fibered.*

**3.** *The inverse image of a  $B(D^2, id, q)$  piece is a disjoint union of pieces of type  $B(D^2, id, q)$ .*

*Proof.* Recall that by the Very Thin Zone Lemma 3.3, the projection  $\ell: W_j \rightarrow V$  has bounded local bilipschitz constant outside a very thin neighbourhood of the polar  $\Pi_j$ . Since the image  $\Delta_j = \pi(\Pi_j)$  lies only in D-pieces of the decomposition of  $V$ , the first two parts of the lemma are clear: each piece is an unbranched cover of the relevant piece of  $V$ , with metric bilipschitz equivalent to the lifted metric.

The third part is also clear if the piece in  $W_j$  is a bilipschitz cover of its image piece of type  $B(D^2, id, q)$ , for example, if the latter does not contain a component of the polar. Otherwise the intersection of the piece in  $W_j$  with each plane  $z_1 = x_0$  is a disk or disjoint union of disks, each of which is a double branched cover of  $D' \cap \{x = x_0\}$ . In this case we have a very small disk  $D'' \subset D'$  given by Corollary 3.7 outside of which the cover is uniformly bilipschitz, and a slight modification of [4, Lemma 2.5] shows that the branched cover of  $D''$  is uniformly bilipschitz equivalent to a flat disk of twice the circumference. The result follows.  $\square$

At this point we have constructed a decomposition of  $W_j$  into “model pieces” but it is not minimal. We will next describe how to simplify it step by step, leading to a decomposition equivalent to the  $W_j$  part of the one described in Section 11.

### 13. BILIPSCHITZ EQUIVALENCE WITH THE MODEL

We will start with the above non-minimal decomposition of  $W_j$  into model pieces and then simplify it until it is minimal. This will use the following trivial lemma, which gives rules for simplifying a decomposition into model pieces. The reader can easily add more rules; we intentionally list only the ones we use.

**Lemma 13.1.** *In this lemma  $\cong$  means bilipschitz equivalence and  $\cup$  represents gluing along appropriate boundary components by an isometry.*

- (1)  $B(D^2, \phi, q) \cong B(D^2, id, q)$ ;  $B(S^1 \times I, \phi, q) \cong B(S^1 \times I, id, q)$ ;
- (2)  $A(q, q') \cup A(q', q'') \cong A(q, q'')$ ;
- (3)  $B(S^1 \times I, id, q) \cup A(q, q') \cong A(q, q')$ ;
- (4) *If  $F$  is the result of gluing a surface  $F'$  to a disk  $D^2$  along boundary components then  $B(F', \phi|_{F'}, q) \cup B(D^2, \phi|_{D^2}, q) \cong B(F, \phi, q)$ ;*
- (5)  $A(q, q') \cup B(D^2, id, q') \cong B(D^2, id, q)$ .  $\square$

We can associate a decomposition graph  $G_j$  to our constructed decomposition of  $W_j$ , again omitting vertices for  $A(q, q')$  pieces since they are indicated by edges between vertices whose weights  $q$  and  $q'$  satisfy  $q < q'$ . There is an obvious graph homomorphism of  $G_j$  to the tree  $T_j$ , induced by the map  $W_j \rightarrow V$ . There may be several “root vertices” in  $G_j$  (vertices which map to the root vertex of  $T_j$ ); they correspond with the intersections of  $W_j$  with thick parts. We direct the edges of  $T_j$  away from the root, and this induces a directed graph structure on  $G_j$ . The

$q$ -weights are non-decreasing along directed edges, and equal along an edge only if the second vertex corresponds to a  $B(D^2, id, q)$  piece.

Starting at the terminal vertices of  $G_j$ , corresponding to “innermost” pieces of  $W_j$ , we apply the rules of the above lemma to amalgamate pieces, simultaneously simplifying the graph  $G_j$ . Thus the first step eliminates the leaves of  $G_j$  and absorbs the corresponding  $D$ -type pieces, but of course, new  $D$ -type pieces can be created in the process. If, during the process, a  $B(S^1 \times I, id, q)$  piece is created for which all adjacent edges of the corresponding vertex of  $G_j$  are incoming, we designate it a “special annulus” and do not apply any further rule to it (the only one possible would be (3)).

At each step of the process there is at least one piece of type  $A(q, q')$  between any two  $B(F, \phi, q)$ -type pieces, except possibly when one of the latter is of type  $B(D^2, id, q)$ , in which case it will be absorbed in the next step. It follows that the process only stops when there is no  $B(D^2, id, q)$  piece left, no pieces of type  $B(S^1 \times I, id, q)$  which are not special annular, and no pairs of adjacent pieces of type  $A(q, q')$ .

The following lemma clarifies where annular pieces of the form  $B(S^1 \times I, id, q)$  can arise during the above procedure.

**Lemma 13.2.** *If an annular piece of type  $B(S^1 \times I, id, q)$  arises during the above procedure it is either an unbranched cover of an annular region in  $V$  or it is a branched cover of a region of type  $B(D^2, id, q)$ . In the former case it will be absorbed by a move (3), while in the latter case it is a special annular region.*

*Proof.* For the piece to be annular its intersection with a Milnor fiber (i.e., intersection with  $\{(z_1 = x_0)\}$ ) must be a union of annuli  $S^1 \times I$ . Euler characteristic shows that an annulus can branched cover only an annulus (with no branching) or a disk. The two possibilities give the two cases in the lemma.  $\square$

**Lemma 13.3.** *After performing the above reduction the graph  $G_j$ , minus its root vertices, is the part corresponding to the thin zone  $Z_j$  of the graph  $\Gamma_0$  of Theorem 1.9 and Section 10.*

*Proof.* We need to show the following:

- (i) If one ignores the annular and special annular pieces the decomposition is the minimal decomposition of  $Z_j^{(\epsilon)}$  into Seifert fibered pieces;
- (ii) there is a special annular piece between two Seifert fibered pieces if and only if the strict transform of the polar meets the corresponding string of rational curves in the resolution graph.

For (i), note that the JSJ decomposition of a thin zone is characterized by the fact that the pieces are not annular and the Seifert fibrations of adjacent pieces do not match up to isotopy on the common torus.

For pieces which do not have a special annular piece between them this is clear: The Seifert fibrations run parallel to the curves of Puiseux approximations to the branches of the  $\Delta_j$  and are determined therefore by the weights  $q$ ; two adjacent pieces with no special annular piece between them are separated by an  $A(q, q')$  and, since  $q \neq q'$ , the fibrations do not match.

For pieces with a special annular piece between them it is also not hard to see. In this case there is an annular region between them which is composed of pieces  $A(q_1, q')$  and  $A(q_2, q')$  glued to a  $B(S^1 \times I, id, q')$  between them. We claim the

mismatch of Seifert fibrations given by  $A(q_1, q')$  and  $A(q_2, q')$  accumulate rather than cancel. A geometric approach is to consider an arc in the Milnor fiber  $W_j \cap \{z_1 = \epsilon e^{i\theta}\}$  from an intersection of a Seifert fiber of the one piece to an intersection of the Seifert fiber of the other, and watch what happens to this arc as one swings the Milnor fiber through increasing  $\theta$ , keeping the arc on the Milnor fiber and its ends on their respective Seifert fibers. If the Seifert fibrations were parallel the arc would have constant length. It passes through the special annulus, and we can assume it does this efficiently, so that its image in the image disk  $V \cap \{z_1 = x_0\}$  enters near a branch point, circles the branch point, and exits. The branch points in this disk are rotating faster than the endpoints of the arc since  $q' > q_1$  and  $q' > q_2$ , so the curve must stretch (see Figure 6).

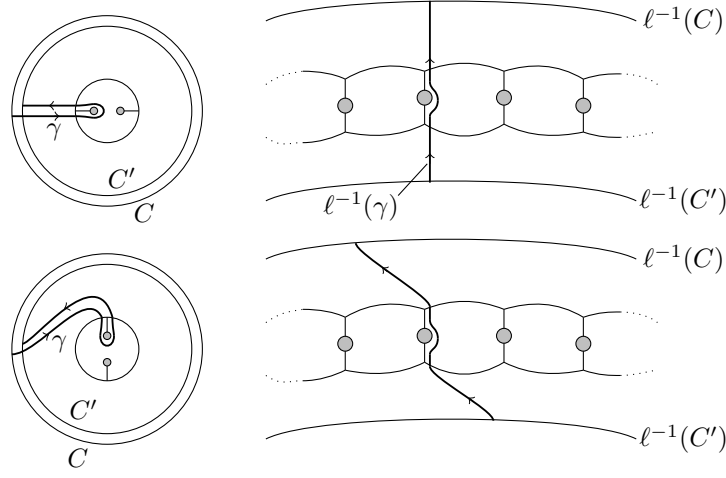


FIGURE 6. Non-matching of Seifert fibers across a special annular piece.

We have proved the correspondence between the non-annular pieces of our decomposition and JSJ-components, and hence with  $\mathcal{T}$ -nodes in  $\Gamma$ . The correspondence (ii) can now be seen as follows. A string between nodes in  $\Gamma$  for which the polar meets an exceptional curve corresponds to an annulus of the Nielsen decomposition of the Milnor fiber (see Remark 7.6) which meets the polar. This means that the annulus covers its image in  $V \cap \{z = \epsilon\}$  with non-trivial branching. By Lemma 13.2 this means the image is a disk, so the annulus is the Milnor fiber of a special annulus.  $\square$

**Remark 13.4.** We can apply the argument of this section to a bamboo attached to an  $\mathcal{L}$ -node instead of a Tjurina component. The reduction process reduces the carrousel to a single  $B(D^2, id, 1)$ , proving part (3) of 6.1. This completes the proof in Section 6 that such a bamboo does not affect conical structure of the thick piece.

If we amalgamate the graphs  $G_j$  by identifying root vertices which correspond to the same thick zone then Lemma 13.3 implies that we get the graph  $\Gamma_0$  of Theorem 1.9 and Section 10. It is the decomposition graph for the decomposition of  $X \cap B_{\epsilon_0}$  into the pieces of the decompositions of the  $W_j$ 's together with the closures of the components of  $(X \cap B_{\epsilon_0}) \setminus \bigcup_j W_j$ .



The vertex-weights  $q_\nu$  are the  $q$ 's of the model pieces of this constructed decomposition. They are the last data we needed to assemble to complete the data of Theorem 1.9.

This decomposition of  $X \cap B_{\epsilon_0}$  into model pieces matches the construction of the model  $\hat{X}$  in Section 11, so we have shown:

**Corollary 13.5.** *The bilipschitz model  $\hat{X}$  constructed in Section 11 using the data we have assembled for Theorem 1.9 is bilipschitz homeomorphic to  $X \cap B_{\epsilon_0}$ .  $\square$*

This corollary completes the proof of half of Theorem 1.9. It remains to show that the data of that theorem are bilipschitz invariants.

**Remark 13.6.** Each vertex  $\nu$  of  $\Gamma_0$  corresponds either to a node of  $\Gamma$  or, in the case of a special annular piece, to a maximal string  $\sigma$  of  $\Gamma$  which contains a vertex corresponding to an exceptional curve which intersect  $\Pi^*$  (we call the minimal substring of  $\sigma$  containing all such vertices an  $\mathcal{A}$ -string, also an  $\mathcal{A}$ -node if it is a single vertex). In discussing examples it is often more convenient to associate the weight  $q_\nu$  with corresponding node or  $\mathcal{A}$ -string of  $\Gamma$ .

Any rate  $q_\nu$  is either 1 or is a characteristic exponent of a branch of the discriminant curve  $\Delta$ . But in general, not all characteristic exponents appear as rates.

For example, the singularity  $(X, 0) \subset (\mathbb{C}^3, 0)$  with equation  $x^3 + y^4 + z^4$  is metrically conical (see 7.12), so the only rate  $q_\nu$  is 1 at the single  $\mathcal{L}$ -node. But the discriminant curve of a generic linear projection consists of four transversal cusps each with Puiseux exponent  $3/2$ .

There are also examples where all characteristic exponents of  $\Delta$  appear as rates  $q_\nu$  of  $\mathcal{T}$ -nodes or  $\mathcal{A}$ -strings. This is the case for any  $(X, 0)$  with equation  $z^2 - f(x, y) = 0$  where  $f$  is irreducible. Indeed, let  $\{(r_k, q_k)\}_{k=1}^s$  be the set of Puiseux pairs of  $f$  (see [9, p. 49]), i.e., the characteristic Puiseux exponents of the curve  $f = 0$  are the rational numbers  $p_k = \frac{q_k}{r_1 \dots r_k}$ . The projection  $\ell = (x, y)$  is generic and its discriminant curve is  $\{f = 0\}$ . By Propositions 4.1 and 4.2 of [26], for any  $k = 1 \dots, s-1$ , each connected component of  $\ell^{-1}(B_k)$  gives rise to a  $\mathcal{T}$ -node of  $\Gamma$  with rate  $p_k$ . Moreover, either  $r_s \neq 2$ , and then  $\ell^{-1}(B_s)$  gives rise to a  $\mathcal{T}$ -node with rate  $p_s$ , or  $r_s = 2$ , and then  $\ell^{-1}(B_s)$  gives rise to a  $\mathcal{A}$ -node with rate  $p_s$ .

#### 14. BILIPSCHITZ INVARIANCE OF THE DATA

In this section, we prove that the data (1), (2) and (3) of Theorem 1.9 are determined by the bilipschitz geometry of  $(X, 0)$ .

We first consider the refined decomposition of  $(X, 0)$  presented in Section 10, which is part (1) of the data of the Classification Theorem 1.9:

$$X^{(\epsilon_0)} = \bigcup_{\nu \in \mathcal{N}_\Gamma} M_\nu^{(\epsilon_0)} \cup \bigcup_{\sigma \in \mathcal{S}_\Gamma} A_\sigma^{(\epsilon_0)}$$

**Lemma 14.1.** *The bilipschitz geometry of  $(X, 0)$  determines, up to isotopy, the above decomposition.*

*Proof of lemma.* The thick-thin decomposition  $(X, 0) = \bigcup_{i=1}^r (Y_i, 0) \cup \bigcup_{j=1}^s (Z_j, 0)$  is determined up to isotopy by the bilipschitz geometry of  $(X, 0)$  (Section 8). For each  $\mathcal{L}$ -node  $\nu$ , the associated thick piece  $Y_\nu$  is defined by  $Y_\nu = \pi(N(\Gamma_\nu))$  (Section 2). Therefore the link  $M_\nu^{(\epsilon_0)}$ , which coincides with  $Y_\nu^{(\epsilon_0)}$  up to a collar neighbourhood, is determined by the bilipschitz geometry. For each Tjurina component  $\Gamma_j$  of  $\Gamma$ ,

the pieces  $M_\nu$  corresponding to  $\mathcal{T}$ -nodes in  $\Gamma_j$  are exactly the Seifert pieces of the minimal JSJ decomposition of  $Z_j^{(\epsilon_0)}$ , so they are determined by the bilipschitz geometry.

It remains to prove that the special annular pieces are also determined by the bilipschitz geometry. This will be done in Lemma 14.4  $\square$

We next prove the bilipschitz invariance of data (2) of Theorem 1.9.

**Lemma 14.2.** *The bilipschitz geometry of  $(X, 0)$  determines for each thin zone  $Z_j^{(\epsilon)}$  the foliation of  $Z_j^{(\epsilon)}$  by fibers of  $\zeta_j^{(\epsilon)}$ .*

*Proof.* We begin with a remark: If  $Z \rightarrow S^1$  is a fibration of a compact connected oriented 3-manifold, we consider  $Z$  as a foliated manifold, with compact leaves which are the connected components of the fibers. If the fibration has disconnected fibers, then it is the composition with a covering map  $S^1 \rightarrow S^1$  of a fibration with connected fiber  $F$ . This fibration gives the same foliation (and it is determined up to isotopy by  $F \subset Z$ ). We recall also that the isotopy class of a fibration  $\zeta: Z \rightarrow S^1$  of a 3-manifold is determined up to isotopy by the homotopy class  $[\phi] \in [Z, S^1] = H^1(Z; \mathbb{Z})$  and has connected fibers if and only if this class is primitive. (See e.g., [36].)

According to Proposition 5.1, the fibration  $\zeta_j^{(\epsilon)}: Z_j^{(\epsilon)} \rightarrow S^1_\epsilon$  varies continuously with  $\epsilon$ , and the diameter of the fibers shrinks faster than linearly with  $\epsilon$ . As just described, we can modify  $\zeta_j^{(\epsilon)}$  if necessary to have connected fiber  $F_j$  without changing the foliation by fibers. Any fibration  $\zeta: Z_j^{(\epsilon)} \rightarrow S^1$  generating a different foliation up to isotopy has fibers which map essentially to  $S^1$  by  $\zeta_j^{(\epsilon)}$ , so their diameter cannot shrink super-linearly with  $\epsilon$ . Hence our foliation is determined up to isotopy by the bilipschitz geometry.  $\square$

Recall that a continuous family of essential loops  $\{\gamma_\epsilon: S^1 \rightarrow X^{(\epsilon)}\}_{0 < \epsilon \leq \epsilon_0}$  is a *fast loop* (of the first kind) if the lengths shrink faster than linearly in  $\epsilon$ . If  $\text{length}(\gamma_\epsilon) = O(\epsilon^q)$  we call  $q$  the rate of the fast loop.

**Lemma 14.3.** *For a Tjurina component  $\Gamma_j$  of  $\Gamma$  and a  $\mathcal{T}$ -node  $\nu$  in  $\Gamma_j$  we denote by  $F_\nu$  a fiber of the fibration  $\zeta_\nu^{(\epsilon_0)}: M_\nu^{(\epsilon_0)} \rightarrow S^1$  obtained by restricting  $\zeta_j^{(\epsilon_0)}$  to  $M_\nu^{(\epsilon_0)}$ . Then  $F_\nu$  contains a fast loop of the first kind which is not parallel to  $\partial F_\nu$ . The maximal rate of any such fast loop is  $q_\nu$ , so  $q_\nu$  is a bilipschitz invariant.*

*Proof.* Note that a fast loop can only exist in a thin zone  $Z_j^{(\epsilon)}$ , and then an argument similar to the proof of the lemma above shows that there is no loss of generality in only considering fast loops which lie in a Milnor fiber of the thin zone. Indeed, a loop which is not homotopic into a Milnor fiber must map essentially to the circle under the fibration  $\phi_j$  and hence cannot shrink faster than linearly.

According to Proposition 7.7, each boundary component of  $F_\nu$  gives a fast loop. Let  $\gamma$  be an essential closed curve in  $F_\nu$  which is not parallel to a boundary component of  $F_\nu$ , and let  $\delta$  be a boundary component. We can choose  $\gamma$  so that, after connecting these curves to a base-point, both closed curves  $\gamma$  and  $\gamma\delta$  are non boundary-parallel. One of them must be essential in  $X^{(\epsilon_0)}$  and thus satisfy the lemma.

Since  $M_\nu$  is of type  $B(F_\nu, \phi, q_\nu)$ , it is clear that every essential curve in  $F_\nu$  yields a fast loop of rate at least  $q_\nu$ . Now let  $\gamma$  be an essential closed curve in  $F_\nu$  which

is not parallel to a boundary component. Then every representative of  $\gamma$  intersects  $F_\nu$ , and there is a lower bound on the length of the portion of such representatives which lie in  $F_\nu$ . Since  $F_\nu^{(\epsilon)}$  shrinks uniformly at rate  $q_\nu$ , it follows that  $q_\nu$  is also an upper bound on the rate of fast loops with  $\gamma_{\epsilon_0} = \gamma$ .  $\square$

**Lemma 14.4.** *The bilipschitz geometry of  $(X, 0)$  determines the special annular pieces  $M_\nu$  and the maximal rate  $q_\nu$  of each such piece  $M_\nu$ .*

*Proof.* Let  $\gamma$  be a boundary component of the fiber  $F_\nu$  for a  $\mathcal{T}$ -node  $\nu$  and  $\nu'$  the adjacent node for that boundary component. Then  $\gamma$  is a fast loop with rate at least  $\max\{q_\nu, q_{\nu'}\}$ . If there is no special annular piece between  $M_\nu$  and  $M_{\nu'}$ , the argument of the previous lemma shows the maximal rate is exactly  $\max\{q_\nu, q_{\nu'}\}$ , while if there is a special annular piece  $M_{\nu''}$ , then it is  $q_{\nu''}$ .  $\square$

Lemmas 14.3 and 14.4 prove bilipschitz invariance of all the  $q_\nu$ 's and complete the proof of Lemma 14.1. So the proof of Theorem 1.9 is complete.

## 15. EXAMPLES

In this section, we describe the bilipschitz geometry for several examples of normal surface singularities  $(X, 0)$ . Namely, for each of them, we give the dual resolution graph  $\Gamma$  of the minimal resolution  $\pi: (\tilde{X}, E) \rightarrow (X, 0)$  considered in Section 10 with the additional data:

- (1') the nodes ( $\mathcal{L}$ -,  $\mathcal{T}$ - and  $\mathcal{A}$ -) represented by black vertices,
- (2') the arrows representing the strict transform of a generic linear form
- (3') the rate  $q_\nu$  weighting each node  $\nu$

The data (1') and (3') are equivalent respectively to (1) and (3) of Theorem 1.9.

The data (2') determines the multiplicities  $m_\nu$  of the generic linear form  $z_1$  along each exceptional curve  $E_\nu$ ,  $\nu \in \Gamma$ . In all the examples treated here, we are in one of the following two situations: either the link  $X^{(\epsilon)}$  is a rational homology sphere or for each node  $\nu \in \Gamma$ ,

$$\gcd(\gcd(m_\nu, m_\mu), \mu \in V_\nu) = 1,$$

where  $V_\nu$  denotes the set of neighbour vertices of  $\nu$  in  $\Gamma$  including arrows (which have multiplicities 1). In these two situations, the multiplicities  $m_\nu$  determine the embedded topology in  $X^{(\epsilon)}$  of the Milnor fibre of  $z_1$ , and then data (2) of Theorem 1.9 (see e.g. [33]).

Recall that the  $\mathcal{L}$ -nodes of  $\Gamma$  are the vertices carrying at least one arrow or, equivalently, having rate 1. The Tjurina components of  $\Gamma$  are the components obtained by removing the  $\mathcal{L}$ -nodes and adjacent edges. Then, according to Section 2 and Theorem 1.6, the thick-thin decomposition  $(X, 0) = (\bigcup(Y_i, 0)) \cup (\bigcup(Z_j, 0))$  of  $(X, 0)$  is read from the graph  $\Gamma$  as follows:

- The thin pieces  $(Z_j, 0)$  of  $(X, 0)$  correspond to the Tjurina components which are not bamboos.
- The thick pieces  $(Y_i, 0)$  of  $(X, 0)$  are in bijection with the  $\mathcal{L}$ -nodes of  $\Gamma$ . They correspond to the connected components of the graph obtained by removing from  $\Gamma$  the Tjurina components which are not bamboos and their adjacent edges.

Each example has been computed as follows: we start by computing the graph  $\Gamma$  with  $\mathcal{L}$ -nodes and arrows. Then for each Tjurina component, we determine the  $\mathcal{A}$ -nodes and the rates at  $\mathcal{A}$ - and  $\mathcal{T}$ -nodes either by studying the Puiseux expansions of the branches of the discriminant curve  $\Delta$  and the cover  $\ell$ , or by determining the strict transform of the polar curve  $\Pi^*$  using the equation of  $X$  and the multiplicities of the coordinates functions in the graph, or by using Hironaka numbers (see Remark 15.3).

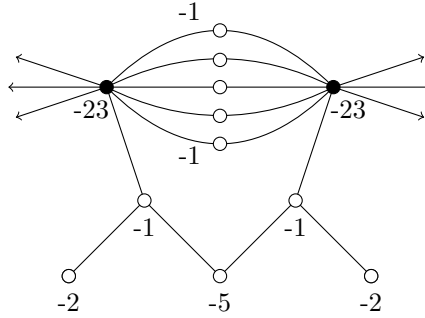
In 15.2 we will treat an example of a superisolated singularity in all detail. We start by presenting the thin-thick decomposition for this family of singularities.

**Example 15.1** (Superisolated singularities). A hypersurface singularity  $(X, 0)$  with equation  $f_d(x, y, z) + f_{d+1}(x, y, z) + \dots = 0$ , where each  $f_k$  is an homogeneous polynomial of degree  $k$ , is *superisolated* if the projective plane curve  $C := \{f_d = 0\} \subset \mathbb{P}^2$  is reduced with isolated singularities  $\{p_i\}_i$  and these points  $p_i$  are not situated on the projective curve  $\{f_{d+1} = 0\}$  (see [18], [24]). Such a singularity is resolved by the blow-up  $\pi_1$  of the origin of  $\mathbb{C}^3$ . Therefore, the thick zones are in bijection with the components of the projectivized tangent cone  $C$ . Moreover, the resolution  $\pi: (\tilde{X}, E) \rightarrow (X, 0)$  introduced in Section 2 is obtained by composing  $\pi_1$  with the minimal resolutions of the plane curve germs  $(C, p_i)$ , and as the curve  $C$  is reduced, no Tjurina component of  $\pi$  is a bamboo. Therefore, the thin zones are in bijection with the points  $p_i$ .

The embedded topological type of  $(X, 0)$  does not depend on the  $f_k$ ,  $k > d$  providing  $f_{d+1} = 0$  does not contain any of the singular points  $p_i$  of  $C$ . The previous arguments show the thin-thick decomposition of  $(X, 0)$  also only depends on  $C$  and does not change when replacing the equation by  $f_d + l^{d+1} = 0$ , where  $l$  is a generic linear form.

For example, taking  $C$  with smooth irreducible components intersecting transversally, we obtain a thick-thin decomposition whose thin zones are all thickened tori, and whose topology comes from the thick pieces (in fact the genus of the irreducible components of  $C$ ) and cycles in the resolution graph.

**Example 15.2**  $((X, 0)$  with equation  $(zx^2 + y^3)(x^3 + zy^2) + z^7 = 0$ ). This is a superisolated singularity and we compute the resolution graph with  $\mathcal{L}$ -nodes and strict transform of the generic linear form by blowing-up the origin and then resolving the singularities of the exceptional divisor. We get two  $\mathcal{L}$ -curves intersecting at five points and one visible Tjurina component in the graph. Blowing-up the five intersection points, we then obtain five additional Tjurina components each consisting of one node between the two  $\mathcal{L}$ -nodes.



The discriminant curve  $\Delta$  of a generic linear projection  $\ell: (X, 0) \rightarrow (C^2, 0)$  has 14 branches and 12 distinct tangent lines  $L_1, \dots, L_{12}$  which decompose as follows:

- three tangent branches  $\delta, \delta', \delta''$  tangent to the same line  $L_1$ , each with single characteristic Puiseux exponent, respectively  $6/5, 6/5$  and  $5/4$ , and Puiseux expansions:

$$\delta: \quad u = av + bv^{6/5} + cv^{7/5} + \dots$$

$$\delta': \quad u = av + b'v^{6/5} + c'v^{7/5} + \dots$$

$$\delta'': \quad u = av + b''v^{5/4} + c''v^{3/2} + \dots$$

- For each  $i = 2, \dots, 6$ , one branch tangent to  $L_i = \{u = a_i v\}$  with  $3/2$  as single characteristic Puiseux exponent:  $u = a_i v + b_i v^{3/2} + \dots$
- 6 branches, each lifting to a component of the polar whose strict transform meets one of the two  $\mathcal{L}$ -curves at a smooth point. So these do not contribute to the bilipschitz geometry.

The lines  $L_2, \dots, L_6$  correspond to the 5 thin zones coming from the 5 one-vertex Tjurina components (compare with Lemma 3.10). These five vertex are thus  $\mathcal{A}$ -nodes with rate equal to the characteristic Puiseux exponent  $3/2$ .

The line  $L_1$  is the projection of the exceptional line tangent to the thin zone  $Z_1$  associated with the big Tjurina component  $\Gamma_1$ . In order to compute the rate  $q_\nu$  at each node  $\nu$  of  $\Gamma_1$ , we would have to study explicitly the restriction of the cover  $\ell$  to  $Z_1$  over a carousel decomposition of its image and the reduction to the bilipschitz model, as in Section 13. The following remark will enable one to circumvent this technical computation.

**Remark 15.3.** Let  $\ell = (z_1, z_2): (X, 0) \rightarrow (\mathbb{C}, 0)$  be a generic linear projection. Denote by  $(u, v) = (z_1, z_2)$  the coordinates in the target  $\mathbb{C}^2$ . Let  $\Gamma_j$  be a Tjurina component of  $\Gamma$  and let  $\gamma$  be a branch of the polar curve of  $\ell$  contained in the thin zone  $Z_j$ . We assume that the branch  $\delta = \ell(\gamma)$  of the discriminant curve has a single characteristic Puiseux exponent  $p_\delta$ . The Puiseux expansion of  $\delta$  is of the form:

$$v = a_1 u + a_2 u^2 + \dots + a_k u^k + bu^{p_\delta} + \dots,$$

where  $k$  denotes the integral part of  $p_\delta$  and where  $b \neq 0$ . We perform the change of variable  $v' = v - \sum_{i=1}^k a_i u^i$ . In other word, we consider the projection  $(z_1, z'_2)$  instead of  $(z_1, z_2)$ , where  $z'_2 = z_2 - \sum_{i=1}^k a_i z_1^i$ . This projection admits the same polar and discriminant curve as  $\ell$ , and in the new coordinates, the Puiseux expansion of  $\delta$  is  $v' = bu^{p_\delta}$ . Let  $\nu$  be a node in  $\Gamma_j$  such that  $\gamma \subset M_\nu$ , i.e.  $q_\nu = p_\delta$ . Then, according to [20, 27], we have:

$$p_\delta = \frac{m_\nu(z'_2)}{m_\nu(z_1)}$$

The quotient  $\frac{m_\nu(z'_2)}{m_\nu(z_1)}$  is called the *Hironaka number* of  $\nu$  (with respect to the projection  $(z_1, z'_2)$ ).

We return to the example. Since each branch  $\delta, \delta'$  and  $\delta''$  has a single characteristic exponent and no inessential exponent before in the expansion, we can apply the remark above. We use  $z'_2 = x + y$ . Let  $E_1, \dots, E_5$  be the exceptional curves associated with the vertices of the big Tjurina component indexed from left to right. We first compute the multiplicities of  $z_1, x$  and  $y$  along the exceptional

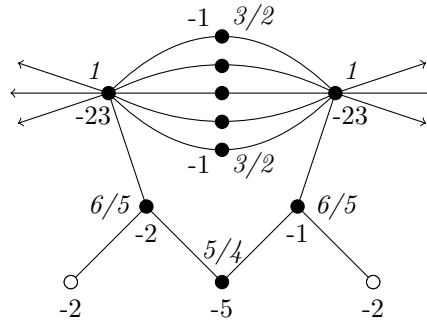
curves  $E_i$ . Then  $z'_2 = x + y$  is a generic linear combination of  $x$  and  $y$  and we obtain its multiplicities as the minimum of that of  $x$  and  $y$  on each vertex:

	$E_1$	$E_2$	$E_3$	$E_4$	$E_5$
$z_1 :$	5	10	4	10	5
$x :$	7	13	5	12	6
$y :$	6	12	5	13	7
$x + y :$	6	12	5	12	6


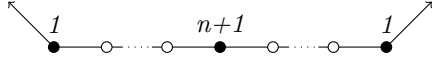
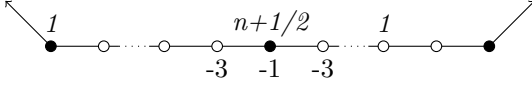
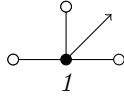
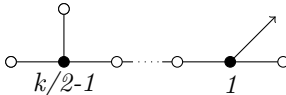
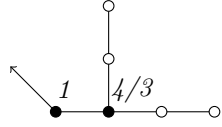
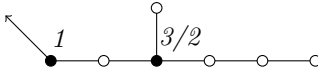
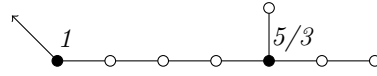
Therefore the Hironaka numbers at the vertices of the Tjurina component  $\Gamma_1$  are:

$E_1$	$E_2$	$E_3$	$E_4$	$E_5$
$6/5$	$6/5$	$5/4$	$6/5$	$6/5$

We thus obtain that the rates at the two  $\mathcal{T}$ -nodes equal  $6/5$ , and that the vertex in the middle is an  $\mathcal{A}$ -node with rate  $5/4$ . The bilipschitz geometry of  $(X, 0)$  is then given by the following graph. The rate at each node is written in *italic*.



**Example 15.4** (Simple singularities). The bilipschitz geometry of the A-D-E singularities is given in the array below. The right column gives the numbers of thin pieces and thick pieces. According to Corollary 7.11, when  $(X, 0)$  doesn't have a thin piece, then it has a single thick piece and  $(X, 0)$  is metrically conical. Otherwise  $(X, 0)$  is not metrically conical.

Singularity	bilipschitz geometry	thick-thin pieces
$A_1$		metrically conical
$A_{2n+1}, n \geq 1$		2 thick, 1 thin
$A_{2n}, n \geq 1$		2 thick, 1 thin
$D_4$		metrically conical
$D_k, k \geq 5$		1 thick, 1 thin
$E_6$		1 thick, 1 thin
$E_7$		1 thick, 1 thin
$E_8$		1 thick, 1 thin

**Example 15.5** (Hirzebruch-Jung singularities). The Hirzebruch-Jung singularities (surface cyclic quotient singularities) were described by Hirzebruch as the normalizations of the singularities  $(Y, 0)$  with equation  $z^p - x^{p-q}y = 0$  in  $\mathbb{C}^3$ , where  $1 \leq q < p$  are coprime positive integers. The link of the normalization  $(X, p)$  of  $(Y, 0)$  is the lens space  $L(p, q)$  (see [12, 14]) and the minimal resolution graph is a bamboo

$$\begin{array}{c} -b_1 \quad -b_2 \quad \dots \quad -b_n \\ \circ \text{---} \circ \text{---} \dots \text{---} \circ \end{array}$$

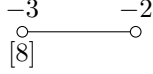
where  $p/q = [b_1, b_2, \dots, b_n]$ . The thin-thick decomposition of  $(X, 0)$  has been already described in the proof of Theorem 7.5: the generic linear form has multiplicity 1 along each  $E_i$ , and the  $\mathcal{L}$ -nodes are the two extremal vertices of the bamboo and any vertex with  $b_i \geq 3$ . To get the adapted resolution graph of section 2 we blow up once between any two adjacent  $\mathcal{L}$ -nodes. Then the subgraph  $\Gamma_j$  associated with a thin piece  $Z_j$  is either a  $(-1)$ -weighted vertex or a maximal string  $\nu_i, \nu_{i+1}, \dots, \nu_k$  of

vertices excluding  $\nu_1, \nu_n$  carrying self intersections  $b_j = -2$ . There are no  $\mathcal{T}$ -nodes and there is an  $\mathcal{A}$ -string in each Tjurina component.

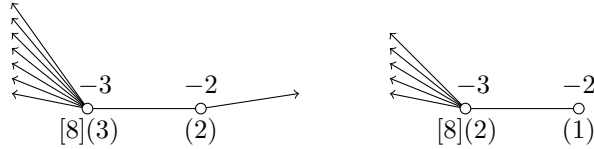
**Example 15.6** (Cusp singularities). Let  $(X, 0)$  be a cusp singularity ([13]). The dual graph of the minimal resolution of  $(X, 0)$  consists of a cycle of rational curves with Euler weights  $\leq -2$  and at least one weight  $\leq -3$ . Since such a singularity is taut, its maximal cycle coincides with its fundamental cycle, and the generic linear form has multiplicity 1 along each irreducible component  $E_i$ . Therefore, the  $\mathcal{L}$ -nodes are the vertices which carry Euler class  $\leq -3$ , and the argument is now similar to the lens space case treated above: we blow up once between any two adjacent  $\mathcal{L}$ -nodes. Then the subgraph  $\Gamma_j$  associated with a thin piece  $Z_j$  is either a  $(-1)$ -weighted vertex or a maximal string  $\nu_i, \nu_{i+1}, \dots, \nu_k$  of vertices carrying weights  $b_j = -2$ . As the distance  $\epsilon$  to the origin goes to zero, we then see the link  $X^{(\epsilon)}$  as a “necklace” of thick zones separated by thin zones, each of the latter vanishing to a circle. Again, there are no  $\mathcal{T}$ -nodes and there is an  $\mathcal{A}$ -string in each Tjurina component.

**Example 15.7** (Briançon-Speder examples). The Briançon-Speder example we will consider is the  $\mu$ -constant family of singularities  $x^5 + z^{15} + y^7 z + txy^6 = 0$  depending on the parameter  $t$ . We will see that the bilipschitz geometry changes very radically when  $t$  becomes 0 (the same is true for the other Briançon-Speder families).

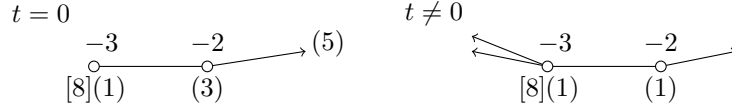
The minimal resolution graph of  $(X, 0)$  is



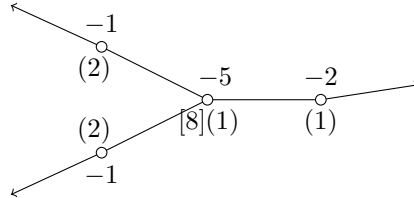
For any  $t$  the curves  $x = 0$  and  $y = 0$  are



The curve  $z = 0$  is

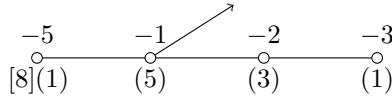


A generic linear form for  $t \neq 0$  is  $z = 0$ , given by the right hand graph above. To resolve the pencil one must blow up twice at the left node, giving three  $\mathcal{L}$ -nodes:

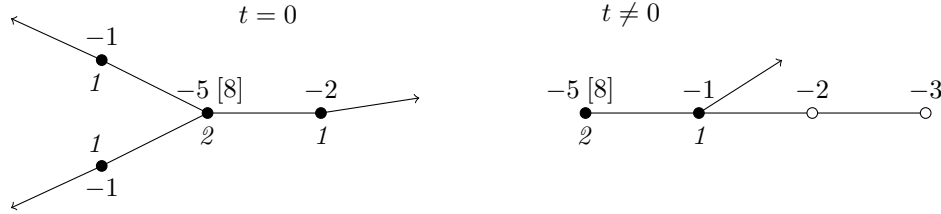


The generic linear for  $t = 0$ , with the pencil resolved, is





So there is just one  $\mathcal{L}$ -node, and it is equal to neither of the original vertices of the resolution. We compute the rate at the  $\mathcal{T}$ -node from the Puiseux expansion of the branches of  $\Delta$  and we obtain the following bilipschitz description:



## REFERENCES

- [1] Andreas Bernig, Alexander Lytchak, Tangent spaces and Gromov-Hausdorff limits of subanalytic spaces, *J. Reine Angew. Math.* **608** (2007), 1–15. 2, 23, 24
- [2] Lev Birbrair, Alexandre Fernandes, Inner metric geometry of complex algebraic surfaces with isolated singularities, *Comm. Pure Appl. Math.* **61** (2008), 1483–1494. 1
- [3] Lev Birbrair, A Fernandez, Walter D Neumann, Bi-Lipschitz geometry of weighted homogeneous surface singularities. *Math. Ann.* **342** (2008), 139–144. 1, 4, 17, 18
- [4] Lev Birbrair, A Fernandez, Walter D Neumann, Bi-Lipschitz geometry of complex surface singularities, *Geometriae Dedicata* **129** (2009), 259–267. 1, 21, 30
- [5] Lev Birbrair, A Fernandez, Walter D Neumann, Separating sets, metric tangent cone and applications for complex algebraic germs, *Selecta Math.* **16**, (2010), 377–391. 1
- [6] Romain Bondil, Discriminant of a generic projection of a minimal normal surface singularity, *Comptes Rendus Mathématique* **337** (2003), 195–200. 8
- [7] Jean-François Boutot, Singularités rationnelles et quotients par les groupes réductifs. *Invent. Math.* **88** (1987), 65–68. 20
- [8] Alan H Durfee, Neighborhoods of algebraic sets. *Trans. Amer. Math. Soc.* **276** (1983), 517–530. 7
- [9] David Eisenbud, Walter D Neumann, *Three dimensional link theory and invariants of plane curves singularities*, Annals of Mathematics Studies 110, Princeton University Press, 1985. 33
- [10] Alexandre Fernandes. Topological equivalence of complex curves and bi-Lipschitz maps, *Michigan Math. J.* **51** (2003), 593–606. 1
- [11] Robert Hardt and Dennis Sullivan, Variation of the Green function on Riemann surfaces and Whitney’s holomorphic stratification conjecture. *Inst. Hautes Études Sci. Publ. Math.* **68** (1988), 115–137 (1989) 1
- [12] Friedrich Hirzebruch, Über vierdimensionale Riemannsche Flächen mehrdeutiger analytischer Funktionen von zwei Veränderlichen. *Math. Ann.* **126** (1953), 1–22. 39
- [13] Friedrich Hirzebruch, Hilbert modular surfaces, *Enseign. Math.* **19** (1973), 183–281. 40
- [14] Friedrich Hirzebruch, Walter D. Neumann, S. S. Koh: Differentiable manifolds and quadratic forms. *Math. Lecture Notes*, vol 4, Dekker, New-York (1972). 39
- [15] W.C. Hsiang, V. Pati,  $L^2$ -cohomology of normal algebraic surfaces. I. *Invent. Math.* **81** (1985), 395–412. 5, 25
- [16] Melvin Hochster, Joel L Roberts, Rings of invariants of reductive groups acting on regular rings are Cohen-Macaulay. *Advances in Math.* **13** (1974) 115–175. 20
- [17] Erich Kähler, Über die Verzweigung einer algebraischen Funktion zweier Veränderlichen in der Umgebung einer singulären Stelle. *Math. Z.* **30** (1929), 188–204. 7
- [18] Ignacio Luengo, The  $\mu$ -constant stratum is not smooth, *Invent. Math.*, **90** (1), 139–152, 1987. 36
- [19] Lê Dũng Tráng, The geometry of the monodromy theorem. C. P. Ramanujama tribute, *Tata Inst. Fund. Res. Studies in Math.*, **8** (Springer, Berlin-New York, 1978) 157–173. 27

- [20] Lê Dũng Tráng, Hélène Maugendre, Claude Weber, Geomtry of critical loci, J. London Math. Soc. **63** (2001) 533–552. 37
- [21] Lê Dũng Tráng, Françoise Michel, Claude Weber, Sur le comportement des polaires associées aux germes de courbes planes. *Compositio Mathematica* **72** (1989), 87–113. 28
- [22] Lê Dũng Tráng, Françoise Michel, Claude Weber, Courbes polaires et topologie des courbes planes. *Ann. Sci. École Norm. Sup.* **24** (1991), 141–169. 27
- [23] Lê Dũng Tráng, Bernard Teissier, Limites d’espaces tangents en géométrie analytique. *Comment. Math. Helv.* **63** (1988) 540–578. 4, 15
- [24] Ignacio Luengo, Alejandro Melle-Hernández, András Némethi, Links and analytic invariants of super- isolated singularities, *J. Algebraic Geom.* **14** (2005), 543–565. 36
- [25] Tadeusz Mostowski, Lipschitz equisingularity, *Dissertationes Math. (Rozprawy Mat.)* **243** (1985), 46pp 1
- [26] Robert Mendris, András Némethi, The link of  $f(x, y) + z^n = 0$  and Zariski’s conjecture, *Compositio Math.* **141** (2005) 502–524. 33
- [27] Françoise Michel, Jacobian curves for normal complex surfaces, *Contemporary Mathematics* **475** (2008) 135–149. 37
- [28] Françoise Michel, Anne Pichon, Claude Weber, The boundary of the Milnor fiber of of some non-isolated singularities, *Osaka J. Math.* **46** (2009), 1–26. 19
- [29] John Milnor. *Singular points of complex hypersurfaces*, *Annals of Mathematics Studies*, **61** (Princeton University Press, Princeton, N.J.; University of Tokyo Press, Tokyo 1968) 7
- [30] Masayoshi Nagase, Remarks on the  $L^2$ -cohomology of singular algebraic surfaces. *J. Math. Soc. Japan* **41** (1989), 97–116. 5, 25
- [31] Walter D Neumann, A calculus for plumbing applied to the topology of complex surface singularities and degenerating complex curves, *Trans. Amer. Math. Soc.* **268** (1981), 299–343. 19
- [32] F. Pham and B. Teissier. Fractions Lipschitziennes d’une algebre analytique complexe et saturation de Zariski. *Prépublications Ecole Polytechnique* No. M17.0669 (1969). 1
- [33] Anne Pichon, Fibrations sur le cercle et surfaces complexes, *Ann. Inst. Fourier (Grenoble)* **51** (2001), 337–374. 18, 35
- [34] Jawad Snoussi, Limites d’espaces tangents à une surface normale. *Comment. Math. Helv.* **76** (2001), 61–88. 4, 5, 6, 8, 15
- [35] Mark Spivakovsky, Sandwiched singularities and desingularization of surfaces by normalized Nash transformations. *Ann. of Math.* **131** (1990), 411–491. 6
- [36] John Stallings, On fibering certain 3-manifolds, in *Topology of 3-manifolds and Related Topics* (Ed. M. K. Fort, Jr.) (Prentice Hall, 1962) 95–99. 23, 34
- [37] Guillaume Valette, The link of the germ of a semi-algebraic metric space. *Proc. Amer. Math. Soc.* **135** (2007), 3083–3090. 16
- [38] Friedhelm Waldhausen, On irreducible 3-manifolds which are sufficiently large, *Annals of Math.* **87** (1968) 56–88. 23

DEPARTAMENTO DE MATEMÁTICA, UNIVERSIDADE FEDERAL DO CEARÁ (UFC), CAMPUS DO PICICI, BLOCO 914, CEP. 60455-760. FORTALEZA-CE, BRASIL

*E-mail address:* birb@ufc.br

DEPARTMENT OF MATHEMATICS, BARNARD COLLEGE, COLUMBIA UNIVERSITY, 2009 BROADWAY MC4424, NEW YORK, NY 10027, USA

*E-mail address:* neumann@math.columbia.edu

INSTITUT DE MATHÉMATIQUES DE LUMINY, UMR 6206 CNRS, AIX-MARSEILLE UNIVERSITÉ, CAMPUS DE LUMINY - CASE 907, 13288 MARSEILLE CEDEX 9, FRANCE

*E-mail address:* pichon@iml.univ-mrs.fr